AD_____

Award Number: DAMD17-03-1-0366

TITLE: The Protein Kinase, RSK2, A Novel Drug Target for Breast Cancer

PRINCIPAL INVESTIGATOR: Deborah A. Lannigan, Ph.D.

CONTRACTING ORGANIZATION: University of Virginia
Charlottesville, VA 22908

REPORT DATE: May 2005

TYPE OF REPORT: Annual

PREPARED FOR: U.S. Army Medical Research and Materiel Command
Fort Detrick, Maryland 21702-5012

REPORT DOCUMENTATION PAGE

Form Approved
OMB No. 074-0188

1. AGENCY USE ONLY (Leave blank)	2. REPORT DATE	3. REPORT TYPE AND DATES COVERED
	May 2005	Annual (1 May 2004 - 30 Apr 2005)

4. TITLE AND SUBTITLE
The Protein Kinase, RSK2, A Novel Drug Target for Breast Cancer

5. FUNDING NUMBERS
DAMD17-03-1-0366

6. AUTHOR(S)
Deborah A. Lannigan, Ph.D.

7. PERFORMING ORGANIZATION NAME(S) AND ADDRESS(ES)
University of Virginia
Charlottesville, VA 22908

E-Mail: Dal5f@virginia.edu

8. PERFORMING ORGANIZATION REPORT NUMBER

9. SPONSORING / MONITORING AGENCY NAME(S) AND ADDRESS(ES)
U.S. Army Medical Research and Materiel Command
Fort Detrick, Maryland 21702-5012

10. SPONSORING / MONITORING AGENCY REPORT NUMBER

11. SUPPLEMENTARY NOTES

12a. DISTRIBUTION / AVAILABILITY STATEMENT
Approved for Public Release; Distribution Unlimited

12b. DISTRIBUTION CODE

13. ABSTRACT (Maximum 200 Words)

The Ser/Thr protein kinase, RSK, is an important downstream effector of MAPK but its roles in breast cancer have not previously been examined. We have now discovered that RSK activity is essential for the growth of the human breast cancer lines, MCF-7 and MDA-MB-231. Taken together, with our observations that the levels of the RSK isoform 2 (RSK2) are higher in ~50% of human breast cancers compared to normal breast tissue suggests that RSK2 is an important drug target for breast cancer. To further test this hypothesis we are developing breast cell lines, that will inducible overexpress RSK2, and transgenic mice that will overexpress RSK2 in the mammary gland. RSK inhibitors, such as SL0101 and its analog, 3Ac-SL0101, should be useful as chemotherapeutic agents for the treatment of breast cancer. The in vivo efficacy of SL0101 and 3Ac-SL0101 to inhibit the growth of MDA-MB-231 tumors is in the process of being evaluated.

14. SUBJECT TERMS
Cell signaling, oncogenesis, drug efficacy

15. NUMBER OF PAGES
43

16. PRICE CODE

17. SECURITY CLASSIFICATION OF REPORT	18. SECURITY CLASSIFICATION OF THIS PAGE	19. SECURITY CLASSIFICATION OF ABSTRACT	20. LIMITATION OF ABSTRACT
Unclassified	Unclassified	Unclassified	Unlimited

Table of Contents

Cover	1
SF 298	2
Introduction	4
Body	4
Key Research Accomplishments	8
Reportable Outcomes	8
Conclusions	8
References	9
Appendices	10

Introduction

We have found that the RSK isoform 2 (RSK2) is overexpressed in human breast cancers compared to normal breast tissue (3). Furthermore, RSK2 is aberrantly regulated in breast cancer cell lines compared to a normal breast line. The importance of RSK2 in the growth of breast cancer has not previously been examined. Therefore, the overall objective of this research project is to evaluate the importance of RSK as a chemotherapeutic target in breast cancer. As part of this evaluation we will determine the efficacy of the RSK-inhibitor, SL0101 to inhibit breast cancer cell growth. We identified this RSK-inhibitor by screening a collection of rare botanical extracts for their ability to inhibit RSK activity. Sl0101 was isolated from the tropical plant *Forsteroinia refracta* and is currently the only known, small-molecule inhibitor, which specifically inhibits RSK *in vitro* and *in vivo* (3).

Body

The research accomplishments associated with each Aim are described below:

Aim 1: Determine whether the RSK2 inhibitor, SL0101, reduces the growth of breast cancer cells in culture or in mouse xenografts.

Year Two

Task 1: Test ability of SL0101 to inhibit growth of breast cells in culture & soft agar.

We have determined that SL0101 specifically inhibits the proliferation of the human breast cancer cell line, MCF-7, producing a cell cycle block in G1 with an efficacy paralleling its ability to inhibit RSK in intact cells (3). Remarkably, SL0101 does not alter the proliferation of a normal breast cell line, MCF-10A even though SL0101 inhibits RSK in these cells. The MCF-7 line is considered to be a model for early stage estrogen receptor alpha (ERα)-positive breast cancer. To investigate whether SL0101 would be effective against more aggressive late stage cancers we determined whether SL0101 would inhibit the growth of MDA-MB-231 cells. SL0101 inhibited the growth of MDA-MB-231 cells with an $EC_{50} \sim 32$ μM compared to ~50 μM for MCF-7 cells (data not shown). Importantly, during the course of these studies we had a novel analog of SL0101 synthesized, 3Ac-SL0101, which was designed to have greater membrane permeability than SL0101 (4). Excitingly, the 3Ac-SL0101 is more effective than SL0101 at inhibiting MDA-MB-231 cells with an EC_{50} of ~15 μM (Fig. 1). The synthesis and characterization of this new highly specific RSK-inhibitor is included in the Appendices. We are currently developing a 96-well soft agar growth assay for use with MDA-MB-231 cells. This assay will allow quantitative determination of anchorage-independent growth and will be useful for determining the effectiveness of SL0101 and 3Ac-SL0101 (2). Taken together, these results are very exciting because there are no targeted therapies for aggressive breast cancer. Thus RSK-inhibitors such as SL0101 and its analogue, 3Ac-SL0101, have the potential for being novel chemotherapeutic agents for both early stage and late stage breast cancer.

As part of our evaluation of SL0101 and 3Ac-SL0101 as chemotherapeutic agents it is essential to identify molecular markers. These molecular markers will be used to demonstrate that the drugs are effective at inhibiting RSK activity *in vivo*. We have identified two such markers. Inhibition of RSK induces a dramatic increase in the phosphorylation of eukaryotic elongation factor 2 (eEF2), an enzyme involved in protein synthesis. Phosphorylation of eEF2 by EF2 kinase (EF2K) inhibits eEF2 activity. RSK phosphorylates and inactivates EF2K in response to mitogenic stimulation, which leads to a decrease in phosphorylation of eEF2 (6). Thus, under conditions in which RSK activity is low, as during serum deprivation, eEF2 is phosphorylated by the active EF2K. As seen in Fig. 2, inhibition of RSK activity by 3Ac-SL0101 treatment induces eEF2 phosphorylation levels even above those induced by serum deprivation. RSK inhibition also reduces the protein levels of the oncogene, cyclin D1 (1). Thus, inhibition of RSK reduces protein synthesis and cell cycle progression in MDA-MB-231 cells.

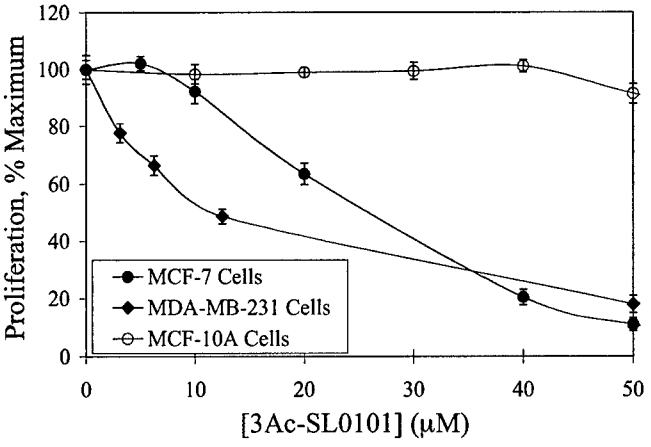

Fig. 1. 3Ac-SL0101 selectively inhibits breast tumor cell proliferation. *MCF-7, MDA-MB-231 and MCF-10A cells were incubated for 48 h in the presence or absence of varying concentrations of 3Ac-SL0101. Measurements were taken at 0 and 48 hr. The data are presented as percent of maximum proliferation.*

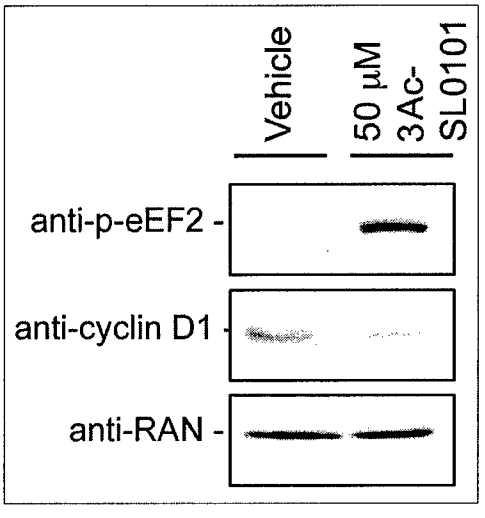

Fig. 2. Alteration in molecular markers with 3Ac-SL0101 treatment. *Serum-deprived MDA-MB-231 cells were treated with vehicle or 50 μM 3Ac-SL0101 for 4 h prior to lysis. Protein concentration of lysates was measured and lysates were electrophoresed, transferred and immunoblotted. Equal loading of lysate is demonstrated by the anti-RAN immunoblot.*

Task 2: Test ability of SL0101 to inhibit tumor formation in nude mice.

Currently, we are evaluating the ability of both SL0101 and 3Ac-SL0101 to inhibit tumor growth *in vivo*. Thus even though 3Ac-SL0101 is more effective than SL0101 in inhibiting MDA-MB-231 cells in tissue culture it may not be the case *in vivo* due to differences in adsorption, distribution, metabolism and excretion parameters. In order to evaluate the efficacy of SL0101 and 3Ac-SL0101 it is important to determine the optimum dose and scheduling of administration, which will maximize the probability of observing an effect of the inhibitor on the tumor while minimizing toxicity to the test animal. We determined the maximum tolerated dosage (MTD) for both compounds using the NCI's general instructions. The compound was administered by i.v. bolus. The MTD of SL0101 was a single dose of 50 mg/kg and for 3Ac-SL0101 was a single dose of 100 mg/kg. These doses should result in peak plasma concentrations that are 30-fold higher for SL0101 and 130-fold higher for 3Ac-SL0101 than that needed to observe inhibition of MDA-MB-231 growth in tissue culture. We also determined that both compounds can be administered at the MTD every fourth day for three treatments (q4dx3) (Fig. 3). This schedule is based on the doubling time of the MDA-MB-231 tumors in xenograft models. The animals did not demonstrate pain or unacceptable levels of distress or exhibit body weight loss of $\geq$20% of their initial weight. Therefore, we have determined the MTD for both compounds.

It is essential to determine the length of time for which a single administration of the MTD is sufficient to maintain an effect on the tumor. If the MTD of the inhibitors is only effective for 24 hrs then the scheduling for administration during the efficacy studies will be every 24 h. However, if a single dose of the MTD maintains an effect on the tumor for up to 96 h, then administration during the efficacy studies will be every 96 h. In order to determine the dosing schedule we had to develop an analytical method to measure SL0101 and 3Ac-SL0101 and their possible metabolites using reverse phase chromatography (Fig. 4). It is predicted that acetylesterases, which are ubiquitous, will cleave the acetyl groups. These compounds elute at distinct regions of the chromatogram and therefore, monitoring metabolism of SL0101 or 3Ac-SL0101 in plasma by observing the disappearance of the SL0101 and 3Ac-SL0101 peak and the appearance of the metabolite peaks will be straightforward. The concentration of SL0101 and 3Ac-SL0101 in the plasma will be determined by comparison with standards.

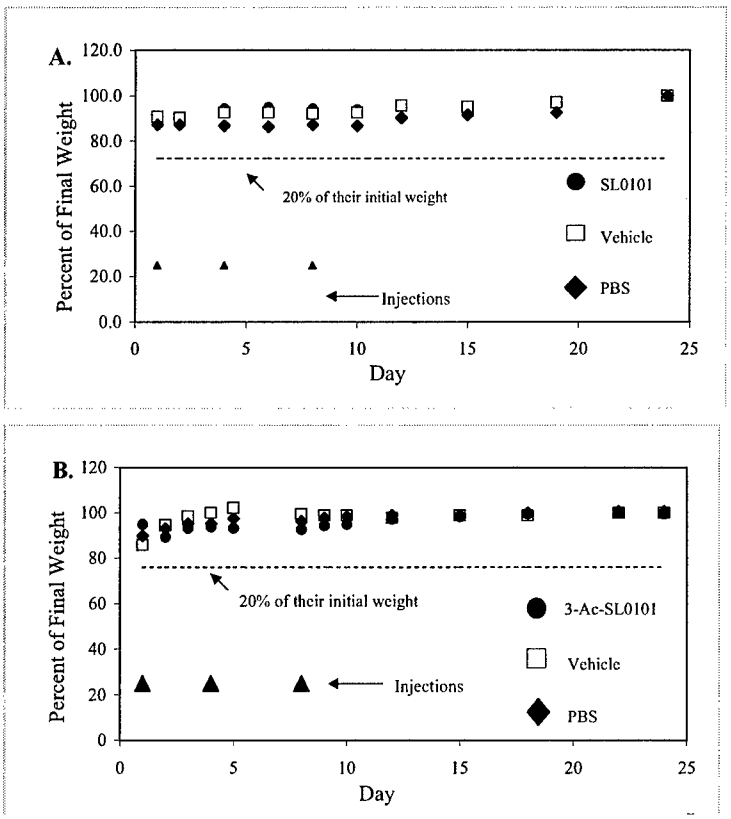

Fig. 3. MTD determination for SL0101 and 3Ac-SL0101. *Female SCID mice were administered The MTD of SL0101 (A) or 3Ac-SL0101 (B) every fourth day for three treatments (q4dx3). The mice were monitored for signs of distress and morbidity. The mice did not demonstrate unacceptable levels of distress nor body weight loss of $\geq$20% of their initial weight.*

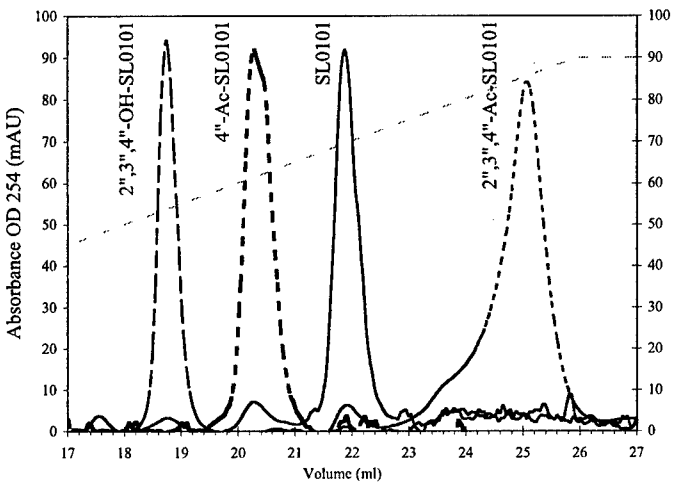

Fig. 4 Reverse phase chromatography of SL0101 and its analogs. *Compounds were individually prepared in the initial mobile phase (1:9 acetonitrile:H_2O). Two hundred microliters of 100 μM was loaded onto the column and eluted with a linear gradient ranging from 1:9 acetonitrile:H_2O to 9:1 acetonitrile:H_2O with UV detection at 254 nm.*

Aim 2: Test whether enhanced RSK2 activity increases breast cancer growth in culture or in mouse xenografts.

Year Two

Task 1 & 2 Develop inducible cell lines & test for growth in culture & soft agar.

The development of an inducible MCF-10A cell line proved to be much more difficult than anticipated. To successfully generate MCF-10A cell lines that will inducible express RSK2 it is necessary to have >50% transfection efficiency. For reasons that are not clear most normal human cell lines are difficult to transfect and we were only able to obtain efficiencies of ~5% using standard methods. We have now developed a novel transfection method in which the transfection efficiency is dramatically improved by maintaining the cells in suspension with the DNA and Lipofectamine 2000. We are now able to obtain transfection efficiencies >70% with this new method.

In the Tet-on system the expression of the gene of interest is regulated by doxycycline in a concentration-dependent manner. However, the transactivator that is commercially available (Clontech) has a number of drawbacks that severely limit its use *in vivo*. Therefore, we obtained a modified Tet-on system from Hillen and colleagues, in which the transactivator has been optimized and has been successfully used *in vivo* (5). We are in the process of generating MCF-10A lines in which the optimized transactivator has been integrated. These cell lines with the optimized transactivator will be a valuable resource to the breast cancer community.

Aim 3: Test whether increased RSK2 activity induces mammary tumor formation in a transgenic mouse model.

Year One & Two

Task 1: Produce & Characterize Transgenic mice.

In the first year we generated an epitope-tagged RSK2 in the inducible mammalian expression vector, pMSG. Although, we had sequenced the insert, RSK2, we decided to sequence the entire vector. Unfortunately, we found that the vector had a deletion in the long terminal repeat (LTR) region that is essential for its function *in vivo*. Fortunately, we were able to obtain a newer generation vector, MKbpAII, from Dr. Rosen (Baylor College of Medicine). In MKbpAII vector the gene of interest is also regulated by the MMTV.

However, this vector has been constructed to place an intron 5' to the gene of interest, which greatly increases mammary gland-specific expression. RSK2 has been inserted into this vector and sequencing of the entire vector is underway.

Key Research Accomplishments

- Discovered that SL0101 inhibits the growth of an aggressive breast cancer line, MDA-MB-231.
- Discovered a novel synthetic analog of SL0101, 3Ac-SL0101, which is more effective at inhibiting the growth of the MDA-MB-231 line than SL0101. These results are extremely exciting because there are no targeted therapies for aggressive breast cancer.
- Identified key molecular markers, eEF2 and cyclin D1, that will be used to establish that the inhibitors function *in vivo*.
- Developed an analytical method to measure the concentration of SL0101 and 3Ac-SL0101 *in vivo*.
- Determined the MTD for SL0101 and 3Ac-SL0101 in mice.
- Developing inducible MCF-10A lines, in which an optimized transactivator is stably integrated. These lines will be valuable resources to the breast cancer research community.

Reportable Outcomes

Manuscripts: Smith, J.A., Poteet-Smith, C.E., Xu, Y., Errington, T.M., Hecht, S.M., Lannigan, D.A. (2005) Identification of the first specific inhibitor of p90 ribosomal S6 kinase (RSK) reveals an unexpected role for RSK in cancer cell proliferation. Cancer Res 65:1027-1034.

Smith, J.A., Reddy, Y.K., Xu, Y., De, S., Holman, N.J., Hecht, S.M. and Lannigan, D.A. (Submitted) Synthesis of the prodrug, kaempferol 3-O-(2",3",4"-tri-O-acetyl-alpha-L-rhamnoside) (3Ac-SL0101), a novel inhibitor of the Ser/Thr protein kinase, RSK.

Grant Submissions: NIH R01 "The RSK2 Protein Kinase-Roles in Breast Cancer"
DoD Breast Cancer IDEA "SL0101, a Potential, Novel Treatment for Late-Stage Breast Cancer"
DoD Breast Cancer Pre-doctoral Fellowship "Importance of RSK2 localization to the nucleus for breast cancer proliferation.

Conclusion

The RSK-specific inhibitor, SL0101 and its analog, 3Ac-SL0101, inhibit the growth of the human breast cancer cell lines, MCF-7 and MDA-MB-231. However, neither compound inhibits the growth of the normal human breast line, MCF-10A. The MCF-7 line is considered to represent an early stage ERα-positive breast cancer line and the MDA-MB-231 line an aggressive late stage breast cancer. Thus RSK-inhibitors have the potential for being novel chemotherapeutic agents for both early stage and late stage breast cancer. These results are of particular interest because there are no targeted therapies for late stage breast cancer.

References

1. **Fu, M., C. Wang, Z. Li, T. Sakamaki, and R. G. Pestell.** 2004. Minireview: Cyclin D1: normal and abnormal functions. Endocrinology **145:**5439-47.
2. **Ke, N., A. Albers, G. Claassen, D. H. Yu, J. E. Chatterton, X. Hu, B. Meyhack, F. Wong-Staal, and Q. X. Li.** 2004. One-week 96-well soft agar growth assay for cancer target validation. Biotechniques **36:**826-8, 830, 832-3.
3. **Smith, J. A., C. E. Poteet-Smith, Y. Xu, T. M. Errington, S. M. Hecht, and D. A. Lannigan.** 2005. Identification of the first specific inhibitor of p90 Ribosomal S6 Kinase (RSK) reveals an unexpected role for RSK in cancer cell proliferation. Cancer Res **65:**1027-1034.
4. **Smith, J. A., K. Yalamareddy, Y. Xu, N. J. Holman, S. M. Hecht, and D. A. Lannigan.** Submitted. Synthesis of the prodrug, kaempferol 3-O-(2", 3", 4"-tri-O-acetyl-a-L-rhamnopyranoside) (3Ac-SL0101), a novel inhibitor of the Ser/Thr protein kinase, RSK.
5. **Urlinger, S., U. Baron, M. Thellmann, M. T. Hasan, H. Bujard, and W. Hillen.** 2000. Exploring the sequence space for tetracycline-dependent transcriptional activators: novel mutations yield expanded range and sensitivity. Proc Natl Acad Sci U S A **97:**7963-8.
6. **Wang, X., W. Li, M. Williams, N. Terada, D. R. Alessi, and C. G. Proud.** 2001. Regulation of elongation factor 2 kinase by p90(RSK1) and p70 S6 kinase. Embo J **20:**4370-9.

Identification of the First Specific Inhibitor of p90 Ribosomal S6 Kinase (RSK) Reveals an Unexpected Role for RSK in Cancer Cell Proliferation

Jeffrey A. Smith,[1,2] Celeste E. Poteet-Smith,[1] Yaming Xu,[3] Timothy M. Errington,[1] Sidney M. Hecht,[3] and Deborah A. Lannigan[1,4]

[1]Center for Cell Signaling, Departments of [2]Pathology and [3]Chemistry, and [4]Microbiology, University of Virginia, Charlottesville, Virginia

Abstract

p90 ribosomal S6 kinase (RSK) is an important downstream effector of mitogen-activated protein kinase, but its biological functions are not well understood. We have now identified the first small-molecule, RSK-specific inhibitor, which we isolated from the tropical plant *Forsteronia refracta*. We have named this novel inhibitor SL0101. SL0101 shows remarkable specificity for RSK. The major determinant of SL0101-binding specificity is the unique ATP-interacting sequence in the amino-terminal kinase domain of RSK. SL0101 inhibits proliferation of the human breast cancer cell line MCF-7, producing a cell cycle block in G_1 phase with an efficacy paralleling its ability to inhibit RSK in intact cells. RNA interference of RSK expression confirmed that RSK regulates MCF-7 proliferation. Interestingly, SL0101 does not alter proliferation of a normal human breast cell line MCF-10A, although SL0101 inhibits RSK in these cells. We show that RSK is overexpressed in ~50% of human breast cancer tissue samples, suggesting that regulation of RSK has been compromised. Thus, we show that RSK has an unexpected role in proliferation of transformed cells and may be a useful new target for chemotherapeutic agents. SL0101 will provide a powerful new tool to dissect the molecular functions of RSK in cancer cells. (Cancer Res 2005; 65(3): 1027-34)

Introduction

The p90 ribosomal S6 kinase (RSK) family are serine/threonine protein kinases that are downstream effectors of mitogen-activated protein kinase (MAPK). In humans, four isoforms have been identified, each the product of distinct genes. The RSK isoforms have similar overall structure with two nonidentical kinase domains separated by a linker region of ~100 amino acids and short amino- and carboxyl-terminal segments. The amino-terminal kinase domain (NTKD) is most closely related to p70 S6 kinase (p70 S6K), whereas the carboxyl-terminal kinase domain (CTKD) is most similar to the calmodulin-dependent protein kinases (1). The regulation of RSK is extremely complex and seems to require a cascade of phosphorylations that result from the action of MAPK, the CTKD of RSK, and 3-phosphoinositide-dependent protein kinase-1 (2–6). RSK contains a docking site for MAPK at its extreme carboxyl terminus, and this docking site is a requirement for specific MAPK phosphorylation of RSK (7, 8). The NTKD is responsible for phosphorylating exogenous substrates and preferentially phosphorylates at serine/threonine residues that lie in RXRXXS/T or RRXS/T motifs (9). The only known function for the CTKD is autophosphorylation of the linker region.

The mechanism of RSK activation has been the subject of many studies, but little progress has been made in understanding the biological functions of RSK. The few substrates identified for RSK include transcription factors like estrogen receptor-α, cyclic AMP response element-binding protein (CREB), c-Fos, and IκBα/nuclear factor-κB (10–14) as well as other kinases, such as glycogen synthase kinase-3, the p34cdc2-inhibitory kinase Myt1, and recently the mitotic checkpoint kinase Bub1 (15–17). The paucity of data concerning key biological roles of RSK in somatic cells results primarily from the difficulty in distinguishing RSK function from those of MAPK itself and of the many other downstream MAPK effectors. This difficulty has arisen because of the lack of RSK-specific inhibitors.

We endeavored to identify a RSK-specific inhibitor by screening botanical extracts using high-throughput screening assays. We have an extensive collection of botanical extracts derived from plants of rare genera. This unique library was collected as part of the original collaboration between the National Cancer Institute and the Department of Agriculture initiated in 1960 for the systematic collection of plants. Herein we describe the discovery, identification, and characterization of the only known small molecule that specifically inhibits RSK *in vitro* and *in vivo*. The inhibitor, which we have named SL0101, was used to uncover a novel and unexpected link between RSK activity and transformed cell proliferation.

Materials and Methods

Kinase Assays. Glutathione *S*-transferase fusion protein (1 μg) containing the sequence RRRLASTNDKG (for serine/threonine kinase assays) or VSVSETDDYAEIIDEEDTFT (for tyrosine kinase assays) was adsorbed in the wells of LumiNunc 96-well polystyrene plates (MaxiSorp surface treatment). The wells were blocked with sterile 3% tryptone in PBS and stored at 4°C for up to 6 months. Kinase (5 nmol/L) in 70 μL of kinase buffer [5 mmol/L -glycerophosphate (pH 7.4), 25 mmol/L HEPES (pH 7.4), 1.5 mmol/L DTT, 30 mmol/L $MgCl_2$, 0.15 mol/L NaCl] was dispensed into each well. Compound at indicated concentrations or vehicle was added, and reactions were initiated by the addition of 30 μL ATP for a final ATP concentration of 10 μmol/L unless indicated otherwise. Reactions were terminated after 10 to 45 minutes by addition of 75 μL 500 mmol/L EDTA (pH 7.5). All assays measured the initial velocity of reaction. After extensive washing of wells, anti-phospho-p140 antibody, a polyclonal phosphospecific antibody developed against the phosphopeptide, CGLA(pS)TND, and horseradish peroxidase (HRP)–conjugated anti-rabbit antibody (211-035-109, Jackson ImmunoResearch Laboratories, West Grove, PA) were used to detect serine phosphorylation of the substrate. Specificity of the

Note: Supplementary data for this article are available at Cancer Research Online (http://cancerres.aacrjournals.org/).

Requests for reprints: Jeffrey A. Smith, Center for Cell Signaling, University of Virginia Health Science Center, Box 800577, Hospital West, 7041 Multistory Building, Charlottesville, VA 22908-0577. Phone: 434-924-1152; Fax: 434-924-1236; E-mail: jas8j@virginia.edu.

anti-phospho-p140 for detection of the phosphorylated peptide is shown in the signal-to-background ratio of the high-throughput screening assays as well as the immunoblots presented in Fig. 5*B* and Supplemental Fig. 3. HRP-conjugated anti-phosphotyrosine antibody (RC20, BD Transduction Laboratories, San Diego, CA) was used for phosphotyrosine detection. HRP activity was measured using Western Lightning Chemiluminescence Reagent (NEL102, Perkin-Elmer Life Sciences, Boston, MA) according to the manufacturer's protocol. Maximum and minimum activity is the relative luminescence detected in the presence of vehicle and 200 mmol/L EDTA, respectively. His-tagged active RSK and focal adhesion kinase (FAK) were expressed in Sf9 cells and purified using NiNTA resin (Qiagen, Valencia, CA). Baculovirus was prepared using the Bac-to-Bac baculovirus expression system (Invitrogen, Carlsbad, CA). Protein kinase A (PKA) was bacterially expressed and activated as described (18). Active MAPK/stress-activated protein kinase-1 (MSK1) and p70 S6K were purchased from Upstate Biotechnology (Charlottesville, VA). Immunoprecipitation and kinase assays were done as described previously (6) using the immobilized GST fusion proteins and ELISA as above.

Cell Culture. For proliferation studies cells were seeded at 2500 to 5000 cells per well in 96 well tissue culture plates in the appropriate medium as described by American Type Culture Collection (Manassas, VA). After 24 hours, the medium was replaced with medium containing compound or vehicle as indicated. Cell viability was measured at indicated time points using CellTiter-Glo assay reagent (Promega, Madison, WI) according to the manufacturer's protocol. For *in vivo* inhibition studies, cells were seeded at 2.5×10^5 cells per well in 12-well cell culture clusters. After 24 hours, the cells were serum starved for 24 hours and then incubated with compound or vehicle for 3 hours before a 30-minute phorbol dibutyrate (PDB) stimulation or a 30-minute stimulation of a cocktail containing 500 nmol/L insulin, 150 ng/mL epidermal growth factor, and 5% FCS (I-E-F). Cells were lysed as described previously (12). The lysates were normalized for total protein, electrophoresed, and immunoblotted. Antibodies used on cell lysates include anti-pan-MAPK (610124) and anti-Ran (610341) from BD Transduction Laboratories; anti-phospho-MAPK (V8031) from Promega; anti-phospho-Akt motif (9611), anti-phospho-CREB (9191), anti-phospho-PKA motif (9621), anti-phospho-protein kinase C (PKC) motif (2261), anti-phospho-S6 (2211), and anti-phosphotyrosine (9411) from Cell Signaling Technology (Beverly, MA); anti-phospho-p140 generated against the phosphopeptide for the HRP-ELISA; and anti-RSK1 (C-21) and anti-RSK2 (E-1) from Santa Cruz Biotechnology (Santa Cruz, CA).

Cell Cycle Analysis. MCF-7 cells were seeded at a density of 1.5×10^5 in 35-mm tissue culture plates and treated the next day for 24 hours with either ethanol, 100 μmol/L SL0101, or 25 μmol/L U0126. Single-cell suspensions were collected, and pellets were fixed in ice-cold ethanol (70%) for 2 hours. After centrifugation of the samples, propidium iodide (50 μg/mL) and RNase (20 units/mL) were added to the pellets for 15 minutes at 37°C. Samples were analyzed by flow cytometry.

Gene Silencing. siGENOME SMARTpool short interfering RNA (siRNA) oligonucleotides to RSK1 (RPS6KA1) and RSK2 (RPS6KA3) mRNA and the siCONTROL nontargeting siRNA I (Dharmacon Research, Inc., Lafayette, CO) were used for the gene silencing studies. Briefly, MCF-7 cells were grown to ~70% confluence and trypsinized. The cells were resuspended at a density of 1×10^6 cells/mL into 2 mL antibiotic-free DMEM containing 10% FCS in a sterile 50 mL tube. Oligonucleotides (200 pmol) were resuspended following the manufacturer's protocols and diluted in 250 μL DMEM and in a separate tube 10 μL LipofectAMINE 2000 was diluted in 250 μL DMEM. The diluted siRNA and diluted LipofectAMINE 2000 were then combined, gently mixed, and allowed to incubate for 20 minutes at room temperature. The siRNA-LipofectAMINE 2000 mixture was added directly to the cells. The cells were centrifuged 4 hours after transfection and resuspended in DMEM containing 10% FCS and antibiotics. The resuspended cells were seeded into 96-well tissue culture plates for proliferation assays and 6-well tissue clusters for determining expression levels. Cells were incubated for 48 hours before initiation of cell viability measurement. The cells for determining expression levels were harvested 72 hours after plating.

Breast Tissue Analysis. These studies complied with the University of Virginia institutional review board and federal requirements. Pathologic specimens were obtained in such a manner that subjects cannot be identified directly or through identifiers linked to the subjects. Frozen human breast tissue samples were examined by frozen section, and areas of cancers were excised from the frozen blocks. Samples of normal and benign breast tissue were obtained from frozen blocks containing abundant epithelium. The tissue was finely ground using mortar and pestle under liquid nitrogen. Ground tissue was added to heated 2× SDS loading buffer and boiled for 3 minutes. Protein concentration of the lysates was measured, and lysates were electrophoresed on SDS-PAGE, immunoblotted, and normalized using anti-Ran antibody. The normalized samples were then electrophoresed and immunoblotted with anti-RSK1, anti-RSK2, and anti-active MAPK antibodies. The intensity of the enhanced chemiluminescence was determined by densitometry and confirmed that data obtained were in the linear range. Each gel contained a sample that permitted normalization between immunoblots. Normal (12 samples) and cancer type (48 samples; lobular and ductal carcinoma) were recorded by the pathology laboratory.

Results and Discussion

Identification of the RSK-Specific Inhibition. High-through put screening ELISAs that produces luminescence as a measure of substrate phosphorylation were developed to identify RSK inhibitors from botanical extracts. The Z' factor of an assay is a statistical characteristic of the quality of the assay with respect to the dynamic range and data variation of the signal measurements (19). A Z' factor of 1 represents the ideal assay with no background and no deviation of signal, whereas a $Z' \leq 0.5$ indicates that the signal window is small to nonexistent. The Z' of the HRP-ELISA developed is ~0.7, indicating a sufficient dynamic range for identifying modulators of kinase activity (Fig. 1*A*). To validate the assay, we determined the IC_{50} of the ATP mimetic H89 for PKA and the IC_{50} of the nonspecific PKC inhibitor Ro 318220 for RSK2, PKA, p70 S6K, and MSK1. The values were consistent with published reports (Fig. 1*B*), which show that the HRP-ELISA we developed is suitable for identifying kinase inhibitors.

Botanical extracts were screened for the presence of a RSK-specific inhibitor. To discriminate extracts containing serine/threonine kinase inhibitors from those containing nuisance compounds, a dual screen of the extracts was done using either a constitutively active RSK2 isoform (RSK2) or the catalytic domain of the tyrosine kinase FAK. One extract that inhibited RSK2 without inhibiting FAK is from *Forsteronia refracta*, a member of the Apocynaceae (dogbane) family found in the South American rainforest (Fig. 2*A*). To determine whether the *F. refracta* extract contained a general serine/threonine kinase inhibitor, activities of the archetypal serine/threonine kinase PKA and of two kinases most closely related to RSK2, p70 S6K and MSK1, were measured in the presence of varying amounts of extract (Fig. 2*B*). Amounts of extract that inhibited RSK2 activity by 90% did not inhibit PKA, p70 S6K, or MSK1 to a greater extent than FAK. Thus, the *F. refracta* extract contains an inhibitor with specificity for RSK2 relative to these other AGC kinase family members.

Fractionation of the extract led to isolation of an active component with an *in vitro* IC_{50} of 89 nmol/L in the presence of 10 μmol/L ATP, the K_m of ATP for RSK (Fig. 3*A* and *B*). Structural determination identified the inhibitor, which we have termed

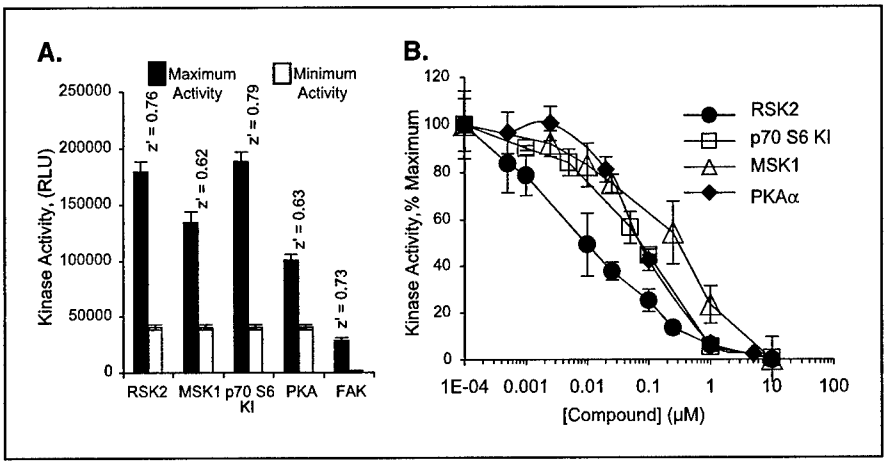

Figure 1. Characterization of the HRP-ELISA. *A*, determination of *Z'* for the HRP-ELISA. Kinase assays were done using immobilized substrate. Reactions were initiated by the addition of 10 μmol/L ATP (final concentration). Reactions were terminated after 10 to 45 minutes. All assays measured the initial reaction velocity. Extent of phosphorylation was determined using phosphospecific antibodies directly labeled with HRP-conjugated or phosphospecific antibodies in combination with HRP-conjugated secondary antibodies. HRP activity was measured as described in Materials and Methods. Maximum and minimum activity is the relative luminescence detected in the presence of vehicle and 200 mmol/L EDTA, respectively. *Columns,* mean (n = 3 in triplicate); *bars,* SD. *B,* inhibition curves generated with the HRP-ELISA. Assays were done as described in *A*. Maximum activity was measured in the presence of vehicle. Inhibition of RSK2, p70 S6K, and MSK1 catalytic activity by Ro 318220 (IC_{50} = 10, 60, and 180 nmol/L, respectively) and inhibition of PKA catalytic activity by H89 (IC_{50} = 60 nmol/L). Kinase activity measured in the presence of the varying concentrations of compound is presented as the percentage of maximum activity. *Points,* mean (n = 2 in triplicate); *bars,* SD.

SL0101, as a kaempferol glycoside (Fig. 3*B*; Supplemental Table 1; ref. 20). The IC_{50} of kaempferol, the flavonoid constituent of SL0101, was determined to be 15 μmol/L for RSK (Fig. 3*A*). Therefore, the rhamnose moiety of SL0101 increases the affinity for RSK by >150-fold. Purified SL0101 is specific for inhibition of RSK activity compared with that of p70 S6K and MSK1 (Fig. 3*C*). SL0101 did not influence the ability of RSK to achieve maximal velocity but altered the K_m of ATP for RSK and is therefore competitive with respect to ATP with a dissociation constant, K_i, of 1 μmol/L (Fig. 3*D*).

SL0101 Interacts with the NTKD of RSK. RSK contains two nonrelated kinase domains in a single polypeptide chain. As stated above, the regulation of RSK is extremely complex and requires activity of both kinase domains. Therefore, inhibition of RSK by SL0101 could occur through interaction with either the NTKD or the CTKD. To determine the domain inhibited by SL0101, we compared the ability of SL0101 to decrease the activity of wild-type or a truncation mutant of RSK2 containing only the NTKD [RSK2(1-389)] (Fig. 4*A*). SL0101 effectively inhibited the isolated RSK2 NTKD.

Because SL0101 is an ATP competitor, we compared the ATP-binding pockets of the AGC kinase family members to identify the determinants of SL0101 specificity. Alignment of the residues forming the ATP-binding pocket of RSK with that of p70 S6K, MSK1, and PKA revealed a difference in the primary structure of the linker region between the two lobes of the catalytic core that contacts the adenosine of ATP (Fig. 4*B*). BLAST analysis indicates that the sequence ^{145}LILDFLRGGDLFT^{157}, the adenosine-interacting loop (AIL), is unique to members of the RSK family. Molecular modeling of residues forming the AIL of the RSK NTKD is shown in Fig. 4*C*. Comparing the AIL models of the RSK NTKD with that of p70 S6K revealed a difference in the dimensions of the pocket created by the AIL. To examine the importance of this region in determining SL0101 specificity, a mutant RSK2 was created in which the p70 S6K-AIL (^{147}LILEYLSGGELFM^{159}) replaced that of RSK2 (RSK2-AILmutant). The RSK2-AILmutant is an active kinase that was inhibited by Ro 318220 to the same extent as was wild-type RSK2; however, SL0101 was much less effective in inhibiting the mutant in comparison with wild-type RSK2 or wild-type RSK1 (Fig. 4*D*). Therefore, the unique AIL of the RSK NTKD is a major determinant for SL0101 specificity. Taken together, these results indicate that inhibition of RSK by

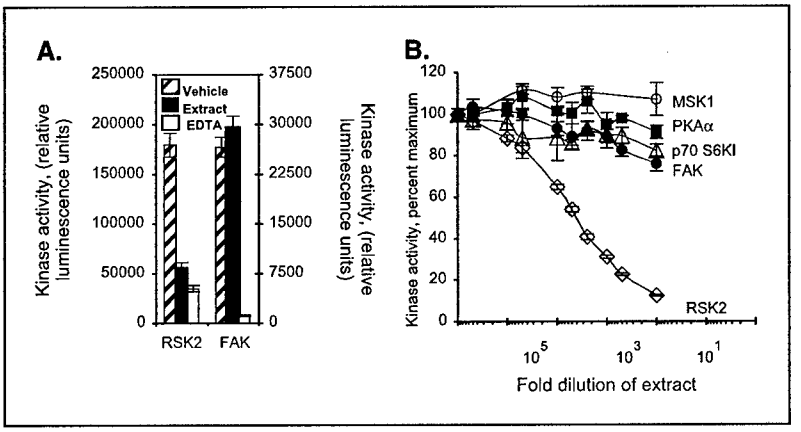

Figure 2. Characterization of the *F. refracta* extract. *A,* effect of the extract on RSK and FAK catalytic activity. Assays were done as described in Fig. 1*A*. Maximum activity was measured in the presence of vehicle. Kinase activity measured in the presence of the extract is presented as the percentage of maximum activity. *Columns,* mean (n = 2 in triplicate); *bars,* SD. *B,* the extract is specific for inhibition of RSK activity. Assays were done as described in Fig. 1*A*. Maximum activity was measured in the presence of vehicle. The nonspecific inhibitor H89 was used as a positive control (data not shown). *Points,* mean (n = 2 in triplicate); *bars,* SD.

SL0101 occurs through competition with ATP for the nucleotide-binding site of the NTKD and further attests to the specificity of SL0101.

SL0101 Is an Effective RSK Inhibitor in Intact Cells. To determine whether SL0101 inhibits RSK in intact cells, phosphorylation of p140, a RSK substrate of unknown function (6), was examined in a human breast cancer cell line MCF-7. Preincubation of cells with 100 μmol/L SL0101 abrogated PDB-induced p140 phosphorylation as did 50 μmol/L U0126, a MAPK/extracellular signal-regulated kinase (ERK) kinase inhibitor (Fig. 5*A*). SL0101 did not affect the phosphorylation of RSK2, as indicated by the reduced electrophoretic mobility of RSK2, nor the activation of MAPK, as detected by the anti-active MAPK antibody (Fig. 5*A*). Therefore, SL0101 does not inhibit upstream kinases necessary for PDB-stimulated RSK activation (i.e., MAPK, MAPK/ERK kinase, Raf, and PKC). These data indicate that SL0101 is membrane permeable and is effective in intact cells. We have shown previously that p140 phosphorylation is not observed in cells treated with the MAPK/ERK kinase inhibitor PD98059. However, p140 phosphorylation does occur in PD98059-treated cells expressing constitutively active RSK2 (6). Thus, p140 is downstream of RSK. To determine whether RSK2 can directly phosphorylate p140, lysates from serum-starved MCF-7 cells treated with vehicle, SL0101, or U0126 and stimulated with PDB or vehicle were transferred to nitrocellulose. The nitrocellulose was incubated in the presence or absence of purified, active, recombinant RSK2 and then immunoblotted. As seen in Fig. 5*B*, RSK can directly phosphorylate immobilized p140. Thus, RSK activity is sufficient for phosphorylation of p140 in intact cells (6) and p140 is phosphorylated by RSK *in vitro*. Taken together, these results suggest that p140 phosphorylation can be used to directly detect RSK activity in intact cells. Additionally, the levels of p140 phosphorylation detected after *in vitro* incubation with active RSK are similar whether the cells were treated with vehicle, SL0101, or U0126. Therefore, the decreased levels of phosphorylated p140 observed in cells treated with SL0101 or U0126 result from reduction of p140 phosphorylation and not alteration of the protein levels. Thus, SL0101 is an effective and specific RSK inhibitor in intact cells.

SL0101 Inhibits Proliferation of MCF-7 Cells. The importance of MAPK to proliferation and oncogenesis is well established (21). However, the role that RSK plays in these processes has not been examined. Therefore, we determined whether SL0101 could inhibit the growth of the human breast cancer cell line MCF-7. Remarkably, SL0101 inhibited proliferation of the MCF-7 line with an efficacy paralleling its ability to inhibit RSK in intact cells but had no effect on the growth of the normal breast cell line MCF-10A (Fig. 6*A* and *B*). Therefore, although SL0101 inhibits RSK activity in MCF-10A cells (Fig. 5*A*), it does not inhibit their growth. Removal of SL0101 after 72 hours resulted in growth of the MCF-7 cells (Fig. 6*C*). Thus, SL0101 is not toxic and preferentially inhibits the growth of the breast cancer cell line relative to that of the normal breast cell line.

Consistent with its antiproliferative effects on cell growth, SL0101 produced a block in the G_1 phase of the cell cycle in MCF-7 cells (Fig. 6*D*). The percentage of cells in G_1 was 38% for vehicle-treated control cells and increased to 67% in SL0101-treated cells with a concomitant decrease in the percentage of cells in both G_2-M

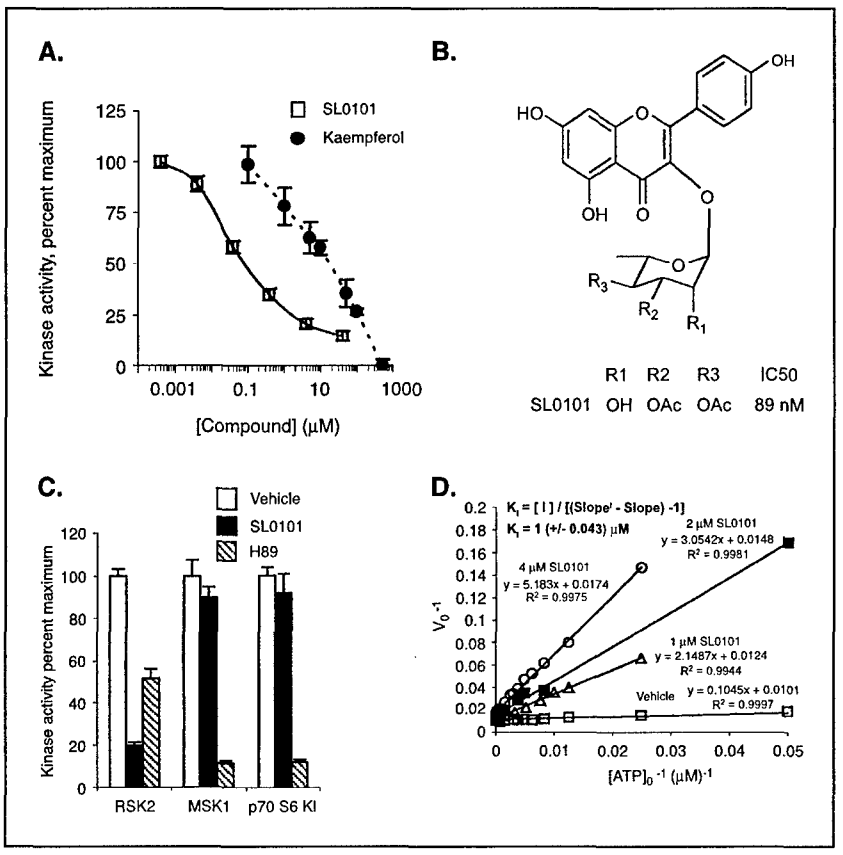

Figure 3. Characterization of SL0101. *A*, inhibition curves of SL0101 and Kaempferol. Potency of purified SL0101 and kaempferol in inhibiting RSK catalytic activity was measured in assays as described in Fig. 1*A*. *Points*, mean (n = 2 in triplicate); *bars*, SD. *B*, structure of SL0101. *C*, SL0101 is specific for inhibition of RSK activity. Kinase assays were done as described in Fig. 1*A* in the presence of vehicle, 2 μmol/L SL0101, or 10 μmol/L H89. *Columns*, mean (n = 3 in triplicate); *bars*, SD. *D*, K_i of SL0101 for RSK2. The inhibitory constant (K_i) of SL0101 for RSK2 was determined by measuring the kinase activity, as described in Fig. 1*A*, in the presence of a constant concentration of SL0101 (1, 2, or 4 μmol/L) and increasing concentrations of ATP. The slope of the plot is increased by the factor $[1 + ([I] / K_i)]$. Thus, the dissociation constant of the enzyme-inhibitor complex was determined to be ~1 μmol/L (n = 2 in triplicate).

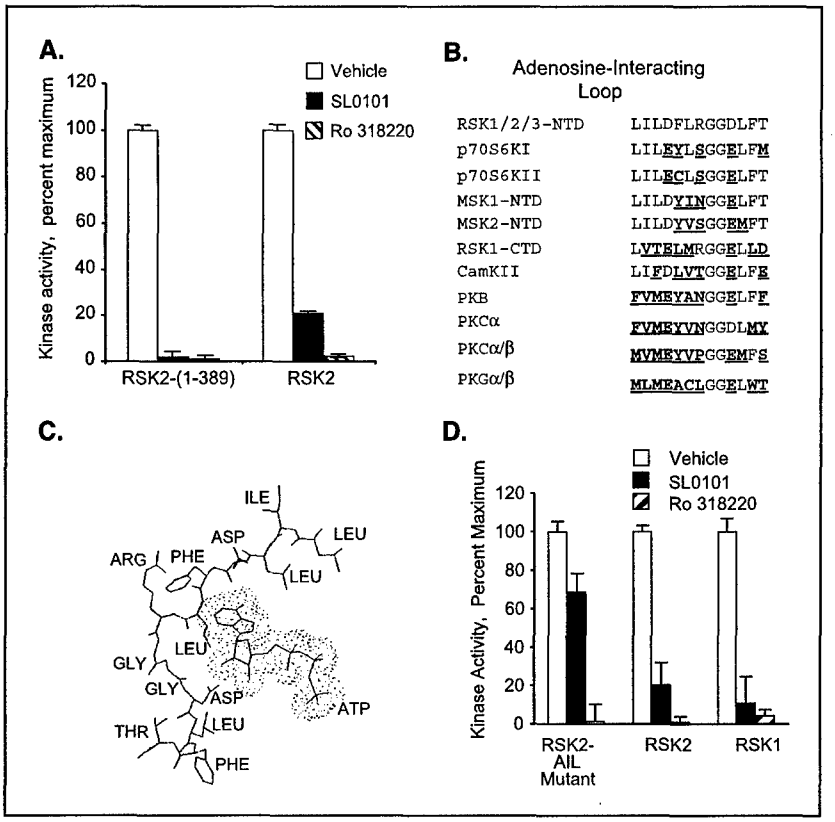

Figure 4. SL0101 inhibits activity of the NTKD. *A*, SL0101 inhibits activity of a RSK2 mutant lacking the CTKD. Hemagglutinin-tagged RSK2 and hemagglutinin-tagged truncation mutant containing the NTKD [RSK2 (1-389)] were transfected into baby hamster kidney 21 cells. Hemagglutinin-tagged proteins were immunoprecipitated from lysates of epidermal growth factor–stimulated cells. Assays were done as described in Fig. 1*A* in the presence of vehicle, 2 μmol/L SL0101, or 2 μmol/L Ro 318220. *Columns*, mean (n = 3 in triplicate); *bars*, SD. *B*, alignment of the primary structure of the AIL from several AGC kinase family members. *Asterisks*, residues in the AIL of RSK predicted to contact ATP based on the crystal structure of PKA; *underlined letters*, residues of the other AGC kinase family members differing from those of RSK. *C*, RSK NTKD AIL is modeled from the crystal structure of PKA. Amino acids are labeled and presented in *stick format*, whereas ATP is presented in *space-filling format*. *D*, RSK NTKD AIL is a major determinant for inhibition by SL0101. Hemagglutinin-tagged proteins were immunoprecipitated from the lysates of epidermal growth factor–stimulated baby hamster kidney 21 cells transfected with the indicated hemagglutinin-tagged constructs. Assays were done as described in Fig. 1*A* in the presence of vehicle, 2 μmol/L SL0101, or 2 μmol/L Ro 318220. *Columns*, mean (n = 3 in triplicate); *bars*, SD.

and S phases. This was also observed for U0126-treated MCF-7 cells (Fig. 6*D*), in agreement with published reports (22). It has been shown that activation of the MAPK pathway is required for the cells to reenter the cell cycle (23). Because SL0101 does not inhibit MAPK activity in intact cells, our data indicate that MAPK activity is not sufficient to initiate reentry into the cell cycle in these cells and that RSK activity is required to pass the G_1 restriction point.

We were able to substantially reduce RSK1 and RSK2 levels using siRNA (Fig. 7*A* and *B*). The data indicate that both RSK1 and RSK2 participate in MCF-7 cell proliferation. Interfering with RSK1 or RSK2 mRNA resulted in a proliferation rate that was 62% and 47% that of cells transfected with control siRNA, respectively. These results strongly support our observations that the RSKs are necessary for MCF-7 proliferation.

As further support of the specificity of SL0101 action, the proliferation of MCF-7 and MCF-10A cells was examined in the presence of other cell-permeable kinase inhibitors (Table 1; Supplemental Fig. 2). Kaempferol, the flavonoid constituent of

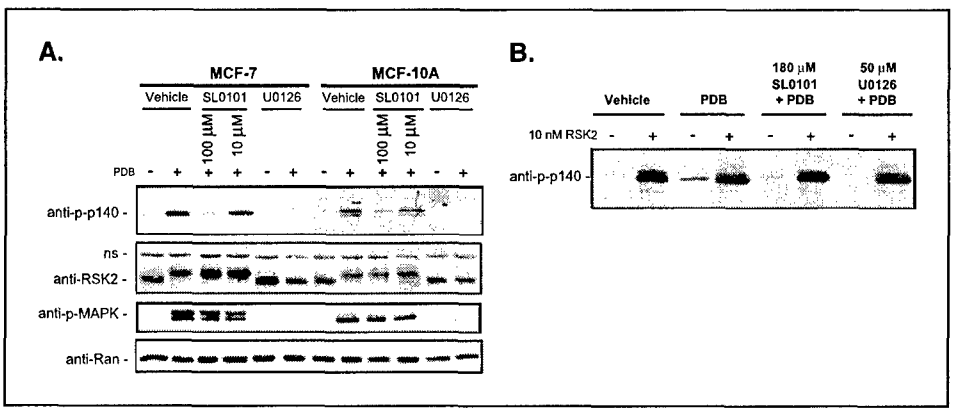

Figure 5. SL0101 is effective in intact cells. *A*, SL0101 inhibits phosphorylation of a RSK substrate in intact cells. MCF-7 and MCF-10A cells were preincubated with vehicle, 50 μmol/L U0126, or the indicated concentration of SL0101 for 3 hours. Cells were treated with 500 nmol/L PDB for 30 minutes before lysis. Protein concentration of lysates was measured, and lysates were electrophoresed, transferred, and immunoblotted. Equal loading of lysate is shown by the anti-Ran immunoblot. *B*, RSK directly phosphorylates pp140 *in vitro*. Serum-starved MCF-7 cells treated with vehicle, SL0101, or U0126 were stimulated with PDB or vehicle. Lysates were subjected to SDS-PAGE and transferred to nitrocellulose in preparation for immunoblotting. The nitrocellulose was cut into strips and incubated in the presence of kinase buffer or kinase buffer containing 10 nmol/L active RSK2. After extensive washing, the strips were placed in a single vessel for immunoblotting.

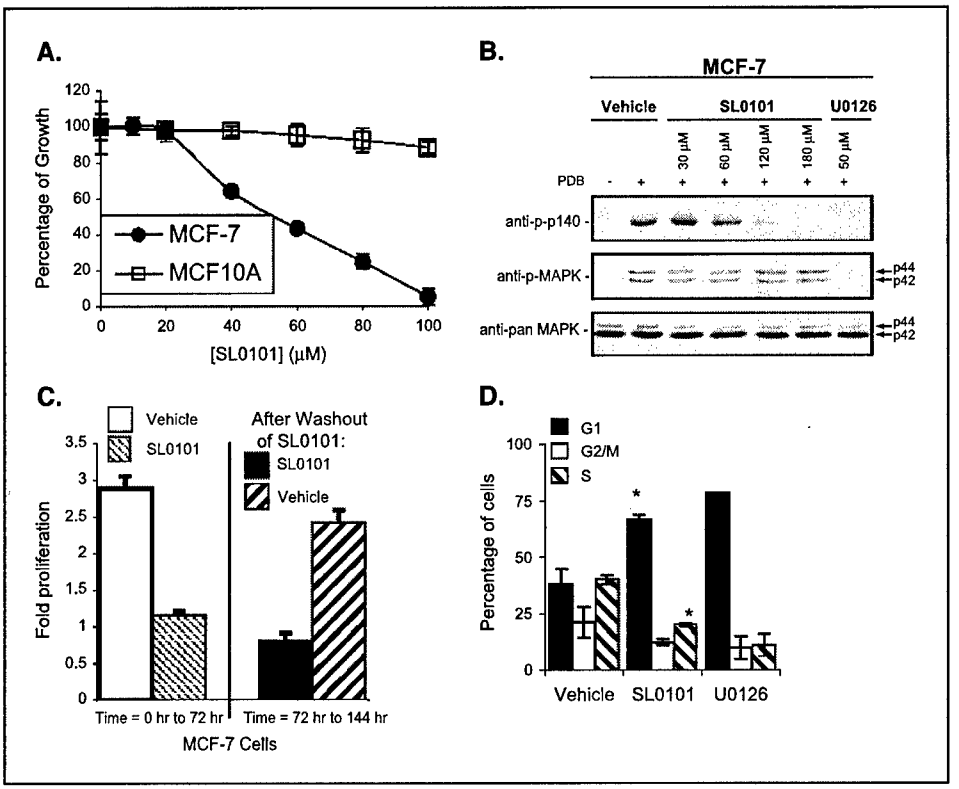

Figure 6. Effect of SL0101 on cell proliferation. *A*, SL0101 selectively inhibits MCF-7 cell proliferation. MCF-7 and MCF-10A cells were treated with vehicle or indicated concentration of SL0101, and cell viability was measured after 48 hours of treatment. Values are fold proliferation as a percentage of that observed with vehicle-treated cells. *Points*, mean (n = 3 in quadruplicate); *bars*, SD. *B*, inhibition of RSK activity by SL0101 parallels its effect on MCF-7 cell proliferation. Serum-starved MCF-7 cells were preincubated with vehicle, 50 μmol/L U0126, or the indicated concentration of SL0101 for 3 hours. Cells were treated with 500 nmol/L PDB for 30 minutes before lysis. Protein concentration of lysates was measured, and lysates were electrophoresed, transferred, and immunoblotted. Equal loading of lysate is shown by the anti-pan-MAPK immunoblot. *C*, MCF-7 cells resume normal growth after removal of SL0101. MCF-7 cells were treated with vehicle or 100 μmol/L SL0101. After 72 hours, the medium was washed out and replaced. Cell viability was measured. In separate plates, cells that had been incubated previously with SL0101 were treated with either 100 μmol/L SL0101 or vehicle and incubated for 72 hours. Cell viability was measured. *Columns*, mean (n = 2 in triplicate); *bars*, SD. *D*, SL0101 causes a G_1-S block in the cell cycle. MCF-7 cells were treated for 24 hours with either vehicle, 100 μmol/L SL0101, or 25 μmol/L U0126 before staining with propidium iodide and flow cytometry analysis. *Columns*, (n = 3); *bars*, SD. *, P = 0.005, Student's t test.

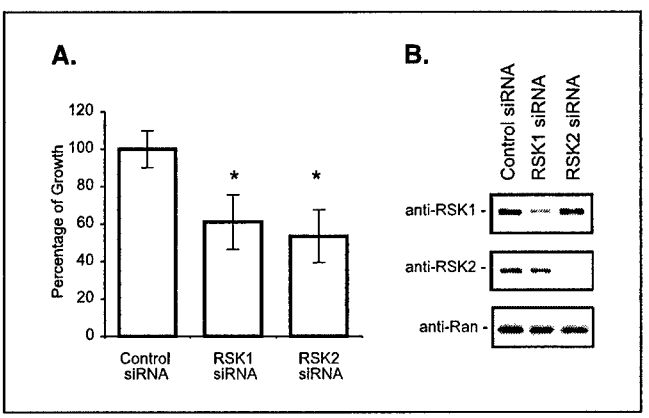

Figure 7. RNA silencing confirms that RSK is important for MCF-7 cell proliferation. *A*, reduction in RSK levels slows the growth of MCF-7 cells. Duplex nontargeting siRNA (*Control*) or RSK1- or RSK2-specific siRNA were transfected into MCF-7 cells. Cell viability was measured at 48 and 72 hours after transfection. Percentage of growth over the 24-hour period is depicted. Fold proliferation of the cells transfected with control siRNA is presented as 100%. *Columns*, mean (n = 2 of 12 replicates); *bars*, SD. *, $P \leq 0.0005$, compared with the control set (Student's t test). *B*, siRNAs reduce RSK protein levels. MCF-7 cells transfected as described in *A* were harvested 72 hours after transfection. Protein levels of RSK1 and RSK2 were examined by immunoblotting. Equal loading of lysate is shown by the anti-Ran immunoblot.

SL0101, slowed the growth of MCF-10A and MCF-7 cells to the same extent. U0126, the MAPK/ERK kinase inhibitor, halted proliferation of both MCF-7 and MCF-10A cells and therefore did not preferentially inhibit growth of the cancer cells. Ro 318220, a potent but nonspecific PKC inhibitor, which inhibits RSK as well as several other AGC kinase family members, also attenuated proliferation of both MCF-7 and MCF-10A cells to the same extent. The PKA inhibitor H89 was more effective at inhibiting the growth of the MCF-7 cells relative to that of the MCF-10A cells. However, concentrations of H89 that inhibited MCF-7 cell growth by ~80% also inhibited the growth of MCF-10A cells by ~40%. Therefore, unlike the action of these other kinase inhibitors, SL0101 selectively inhibits proliferation of the breast cancer cells without affecting the growth of the normal breast cells.

We also compared the phosphorylation patterns from MCF-7 cells preincubated with SL0101 to those from cells pretreated with other cell-permeable kinase inhibitors before stimulation with either PDB or a cocktail of I-E-F. The lysates were immunoblotted with multiple phosphospecific antibodies. As seen in Table 2 and Supplemental Fig. 3, concentrations of SL0101, Kaempferol, U0126, Ro 318220, and H89 that completely inhibit the growth of MCF-7 cells also inhibit phosphorylation of p140. However, all inhibitors,

Table 1. Proliferation of MCF-7 and MCF-10A cells in the presence of commercially available kinase inhibitors

	MCF-7 cells	MCF-10A cells
Kaempferol (μmol/L)		
50	87.6 ± 3.3	93.5 ± 3.7
100	32.3 ± 3.5	45.6 ± 1.6
250	6.1 ± 6.1	0 ± 0.3
U0126 (μmol/L)		
4	83.6 ± 6.3	60.7 ± 3.1
20	43.5 ± 3.5	18.7 ± 1.6
50	−4.5 ± 4.7	5.7 ± 2.6
Ro 318220 (μmol/L)		
0.25	83 ± 0.6	88.2 ± 2.4
0.5	56 ± 2.9	61.5 ± 3.2
1	−31 ± 4	−7 ± 1.3
H89 (μmol/L)		
2	71.2 ± 4.6	96.5 ± 2.2
4	21.5 ± 3	63.9 ± 5.5
8	−62.7 ± 1.7	20.4 ± 0.8

NOTE: MCF-7 and MCF-10A cells in the presence of 10% FCS were treated with vehicle or indicated concentration of compound. Cell viability was measured after 48 hours of treatment. Values given are the fold proliferation as a percentage of that observed with vehicle-treated cells. Negative values indicate that there were fewer viable cells after the 48-hour treatment than at the time treatment was initiated (time = 0 hour). The graphs from which this table was generated are included in Supplemental Fig. 2.

with the exception of SL0101, affected multiple phosphorylation events (Table 2; Supplemental Fig. 3). Whereas SL0101 only altered p140 phosphorylation. These data show that SL0101 does not inhibit PKA, PKC, Akt, or p70 S6K in intact cells. Additionally, SL0101 does not alter the profile of tyrosine phosphorylation in intact cells. Thus, with respect to these commercial kinase inhibitors, SL0101 shows specificity for RSK in intact cells. Interestingly, concentrations of each compound that halt MCF-7 cell growth also inhibit p140 phosphorylation, which suggests that p140 phosphorylation may be linked to proliferation in breast cancer cells.

It has been proposed that among the numerous events involved in tumorigenesis is an increased reliance on the compromised signaling pathway as well as the dormancy of alternative signaling pathways (24, 25). Thus, it seems that MCF-7 cells have become dependent on the RSK pathway, rendering the proliferation of these cells susceptible to inhibition by SL0101. The growth of MCF-10A cells would not be inhibited by SL0101 because intact signaling pathways provide numerous mechanisms for circumventing inhibition of a single signaling event. The involvement of RSK in breast cancer has not been examined previously. Interestingly, we have found that the mean levels of RSK1 and RSK2 in the cancer tissues are statistically higher than that in the normal tissues ($P < 0.05$, Student's t test). As shown by the box-and-whisker plots, ~50% of the cancer tissues displayed RSK1 or RSK2 levels significantly higher than the majority of the normal tissues. (Fig. 8*A*). Analysis of the RSK levels in the breast cancer tissue samples indicates that there is a positive linear relationship between RSK1 and RSK2 levels ($P = 0.0005$; data not shown), suggesting that regulation of both isozyme expression levels has become compromised. However, analysis of active MAPK levels indicates that all cancer tissue samples contained active MAPK, but there is no linear correlation between detectable active MAPK levels and RSK1 or RSK2 expression in the breast cancer tissues (Fig. 8*B*). Thus, the increase in RSK levels is not merely a reflection of overexpression of the various members of the MAPK pathway. We speculate that the growth of tumors, such as breast cancer, will be susceptible to inhibition by SL0101 and that RSK-specific

Table 2. Effect of SL0101 and commercially available kinase inhibitors on phosphorylation patterns in intact cells

Inhibitor	SL0101 (100 μmol/L)	H89 (8 μmol/L)	Kaempferol (250 μmol/L)	Ro318220 (1 μmol/L)	U0126 (50 μmol/L)
Stimulus	PDB/I-E-F	PDB/I-E-F	PDB/I-E-F	PDB/I-E-F	PDB/I-E-F
Phosphoprotein-specific antibodies					
p140	Inh/Inh	Inh/Inh	Inh/Inh	Inh/Inh	Inh/Inh
Ribosomal protein S6	NE/NE	Inh/NE	NE/Inh	Inh/NE	Inh/NE
CREB/activating transcription factor-1	NE/NE	Inh/NE	NE/NE	Inh/NE	Inh/NE
ERK	NE/NE	Inh/NE	NE/Inh	Inh/NE	Inh/Inh
Phospho-motif-specific antibodies					
PKA	NE/NE	Inh/NE	Stim/Stim	Inh/NE	Inh/NE
PKC	NE/NE	Inh/Inh	NE/Inh	Inh/Inh	NE/NE
Akt	NE/NE	Inh/Inh	Stim-Inh/Stim	Inh/Inh	Inh/NE
Phosphotyrosine	NE/NE	NE/NE	NE/Inh	NE/Inh	NE/NE

NOTE: Serum-starved MCF-7 cells were preincubated with vehicle or the indicated concentration of compound for 3 hours. Cells were treated with 500 nmol/L PDB or a cocktail of I-E-F for 30 minutes before lysis. Protein concentration of lysates was measured, and lysates were electrophoresed, transferred, and immunoblotted. Equal loading of lysate was shown by the anti-pan-MAPK immunoblot. Whether the compound altered the protein phosphorylation pattern compared with that observed with vehicle-treated cells is indicated by "Inh" for inhibition, "Stim" for stimulation of protein phosphorylation, or "NE" for no effect on the phosphorylation patterns. The immunoblots from which this table was generated are included in Supplemental Fig. 3.

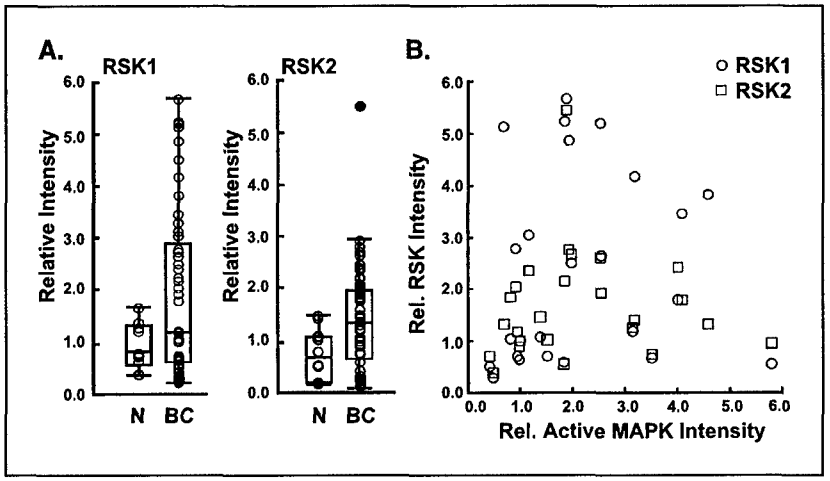

Figure 8. RSK is overexpressed in human breast cancer. Twelve normal (*N*) and 48 cancerous (*BC*; consisting of ductal and lobular carcinoma) breast tissue samples were ground under liquid nitrogen and lysed in SDS loading buffer. Normalized samples were then electrophoresed and immunoblotted with anti-RSK1, anti-RSK2, and anti-active MAPK antibodies. Immunoblots were analyzed by densitometry, and the intensities of RSK (*A*) were plotted as box-and-whisker plots according to Tukey (26). *Bar in the box,* statistical median; *ends of the box,* upper and lower quartiles. *Solid circle in the RSK2 plot,* statistical outlier and not included in the SD. Box-and-whisker plots clearly illustrate the range of the data. Mean of RSK1 and RSK2 levels in the cancer tissue samples and mean in the normal tissue samples are statistically different. $P \leq 0.05$ (Student's *t* test, two-tailed distribution). *B,* active MAPK levels were plotted against RSK1 and RSK2 protein levels measured in the breast cancer tissue. Statistical analysis of active MAPK and RSK levels generates a correlation coefficient that fails to be significant at $P \leq 0.05$; therefore, there is no linear correlation between active MAPK and RSK1 or RSK2 levels.

inhibitors, such as SL0101, may find widespread use as chemotherapeutic agents.

Our studies have uncovered an unexpected link between RSK activity and tumor cell proliferation revealing the value of RSK as a novel drug target. Additionally, we have identified the first RSK-specific inhibitor, SL0101, which will provide a powerful new tool for analyzing RSK function in a variety of biological systems. Additionally, this phytochemical is selectively cytostatic for a human breast cancer cell line without affecting the growth of a normal breast cell line. Thus, RSK-specific inhibitors may be useful as compounds for cancer chemotherapy.

Acknowledgments

Received 5/27/2004; revised 10/19/2004; accepted 11/19/2004.

Grant support: American Chemical Society, Virginia Chapter grant IRG 81-011-17, National Cancer Institute grant CA95335, and Department of Defense grant DAMD17-03-1-0366 USAMRMC.

The costs of publication of this article were defrayed in part by the payment of page charges. This article must therefore be hereby marked advertisement in accordance with 18 U.S.C. Section 1734 solely to indicate this fact.

We thank David L. Brautigan for establishing the infrastructure necessary for the drug discovery program; Ian G. Macara for his invaluable contributions during the research; Gregory P. Riddick for statistical analysis of the human tissue data; J. Thomas Parsons, Ian G. Macara, and Sarah J. Parsons for critical review of the article; and Michael J. Weber for discussions.

References

1. Jones SW, Erikson E, Blenis J, Maller JL, Erikson RL. A *Xenopus* ribosomal S6 kinase has two apparent kinase domains that are each similar to distinct protein kinases. Proc Natl Acad Sci U S A 1988;85:3377–81.
2. Dalby KN, Morrice N, Caudwell FB, Avruch J, Cohen P. Identification of regulatory phosphorylation sites in mitogen-activated protein kinase (MAPK)-activated protein kinase-1a/p90rsk that are inducible by MAPK. J Biol Chem 1998;273:1496–505.
3. Bjorbaek C, Zhao Y, Moller DE. Divergent functional roles for p90rsk kinase domains. J Biol Chem 1995;270:18848–52.
4. Fisher TL, Blenis J. Evidence for two catalytically active kinase domains in pp90rsk. Mol Cell Biol 1996;16:1212–9.
5. Jensen CJ, Buch MB, Krag TO, Hemmings BA, Gammeltoft S, Frodin M. 90-kDa ribosomal S6 kinase is phosphorylated and activated by 3-phosphoinositide-dependent protein kinase-1. J Biol Chem 1999;274:27168–76.
6. Poteet-Smith CE, Smith JA, Lannigan DA, Freed TA, Sturgill TW. Generation of constitutively active p90 ribosomal S6 kinase *in vivo*. Implications for the mitogen-activated protein kinase-activated protein kinase family. J Biol Chem 1999;274:22135–8.
7. Smith JA, Poteet-Smith CE, Malarkey K, Sturgill TW. Identification of an extracellular signal-regulated kinase (ERK) docking site in ribosomal S6 kinase, a sequence critical for activation by ERK *in vivo*. J Biol Chem 1999;274:2893–8.
8. Gavin AC, Nebreda AR. A MAP kinase docking site is required for phosphorylation and activation of p90(rsk)/MAPKAP kinase-1. Curr Biol 1999;9:281–4.
9. Leighton IA, Dalby KN, Caudwell FB, Cohen PT, Cohen P. Comparison of the specificities of p70 S6 kinase and MAPKAP kinase-1 identifies a relatively specific substrate for p70 S6 kinase: the N-terminal kinase domain of MAPKAP kinase-1 is essential for peptide phosphorylation. FEBS Lett 1995;375:289–93.
10. De Cesare D, Jacquot S, Hanauer A, Sassone-Corsi P. Rsk-2 activity is necessary for epidermal growth factor-induced phosphorylation of CREB protein and transcription of c-*fos* gene. Proc Natl Acad Sci U S A 1998;95:12202–7.
11. Ghoda L, Lin X, Greene WC. The 90-kDa ribosomal S6 kinase (pp90rsk) phosphorylates the N-terminal regulatory domain of IκBα and stimulates its degradation *in vitro*. J Biol Chem 1997;272:21281–8.
12. Joel PB, Traish AM, Lannigan DA. Estradiol-induced phosphorylation of serine 118 in the estrogen receptor is independent of p42/p44 mitogen-activated protein kinase. J Biol Chem 1998;273:13317–23.
13. Schouten GJ, Vertegaal AC, Whiteside ST, et al. IκBα is a target for the mitogen-activated 90 kDa ribosomal S6 kinase. EMBO J 1997;16:3133–44.
14. Xing J, Ginty DD, Greenberg ME. Coupling of the RAS-MAPK pathway to gene activation by RSK2, a growth factor-regulated CREB kinase. Science 1996;273:959–63.
15. Sutherland C, Leighton IA, Cohen P. Inactivation of glycogen synthase kinase-3β by phosphorylation: new kinase connections in insulin and growth-factor signalling. Biochem J 1993;296:15–9.
16. MSchwab MS, Roberts BT, Gross SD, et al. Bub1 is activated by the protein kinase p90(Rsk) during *Xenopus* oocyte maturation. Curr Biol 2001;11:141–50.
17. Palmer P, Gavin AC, Nebreda AR. A link between MAP kinase and p34(cdc2)/cyclin B during oocyte maturation: p90(rsk) phosphorylates and inactivates the p34(cdc2) inhibitory kinase Myt1. EMBO J 1998;17:5037–47.
18. Hemmer W, McGlone M, Taylor SS. Recombinant strategies for rapid purification of catalytic subunits of cAMP-dependent protein kinase. Anal Biochem 1997;245:115–22.
19. Zhang J, Chung TDY, Oldenburg KR. A simple statistical parameter for use in evaluation and validation of high throughput screening assays. J Biomol Screen 1999;4:67–73.
20. Matthes HWD, Luu B, Ourisson G. Cytotoxic components of *Zingiber zerumbet*, *Curcuma zedoaria* and *C. domestica*. Phytochemisty 1980;19:2643–50.
21. Sebolt-Leopold JS. Development of anticancer drugs targeting the MAP kinase pathway. Oncogene 2000;19:6594–5.
22. Lobenhofer EK, Huper G, Iglehart JD, Marks JR. Inhibition of mitogen-activated protein kinase and phosphatidylinositol 3-kinase activity in MCF-7 cells prevents estrogen-induced mitogenesis. Cell Growth 2000;11:99–110.
23. Pages G, Lenormand P, L'Allemain G, Chambard JC, Meloche S, Pouyssegur J. Mitogen-activated protein kinases p42mapk and p44mapk are required for fibroblast proliferation. Proc Natl Acad Sci U S A 1993;90:8319–23.
24. Mills GB, Lu Y, Kohn EC. Linking molecular therapeutics to molecular diagnostics: inhibition of the FRAP/RAFT/TOR component of the PI3K pathway preferentially blocks PTEN mutant cells *in vitro* and *in vivo*. Proc Natl Acad Sci U S A 2001;98:10031–3.
25. Neshat MS, Mellinghoff IK, Tran C, et al. Enhanced sensitivity of PTEN-deficient tumors to inhibition of FRAP/mTOR. Proc Natl Acad Sci U S A 2001;98:10314–9.
26. Tukey JW. Explanatory data analysis. Reading (MA): Addison-Wesley; 1977.

Synthesis of the prodrug, kaempferol 3-*O*-(2", 3", 4"-tri-*O*-acetyl-α-L-rhamnopyranoside) (3Ac-SL0101), a novel inhibitor of the Ser/Thr protein kinase, RSK.

Jeffrey A. Smith[*†], Y. Krishna Reddy[#], Yaming Xu[‡], Sidhartha De[¶], Nicholas J. Holman[#], Sidney M. Hecht[‡], and Deborah A. Lannigan[*§]

*Center for Cell Signaling, †Department of Pathology, ‡Department of Chemistry and §Department of Microbiology, University of Virginia, Charlottesville, VA 22908-0577

¶ Luna Innovations, Charlottesville, VA, 22903

Albany Molecular Research Inc., Syracuse Research Center, North Syracuse, NY 13212

Corresponding author: Deborah A. Lannigan

Center for Cell Signaling

Box 800577, Health Sciences Center

University of Virginia

Charlottesville, Virginia 22908-0577

Tel: 434-924-1144; Fax: 434-924-1236

dal5f@virginia.edu

Abstract

We have previously reported the isolation of kaempferol 3-*O*-(3",4"-di-*O*-acetyl-α-L-rhamnopyranoside) from *Forsteronia refracta*. This flavonoid glycoside is specific inhibitor of p90 ribosomal S6 kinase (RSK) with a dissociation constant, K_i, of 1 μM. In intact cells, however, the EC_{50} for inhibition of RSK activity is 50 μM. Therefore, on the assumption that the potency of SL0101 in cells was limited by cellular uptake, we investigated the possibility of improving the potency of SL0101 by synthesis of an analog with an increased octanol-water partition coefficient, LogP. The total synthesis of kaempferol 3-*O*-(2",3","4"-tri-*O*-acetyl-a-L-rhamnopyranoside), referred to as 3Ac-SL0101, was performed. The EC_{50} of 3AC-SL0101 for inhibition of MCF-7 cell proliferation is 25 μM. Increasing the LogP improved the efficacy of the RSK inhibitor by ~2-fold. The improved RSK inhibitor, 3Ac-SL0101, demonstrates the same remarkable specificity for inhibiting RSK catalytic activity in intact cell as SL0101. Thus 3Ac-SL0101 is of interest for further characterization as a potential chemotherapeutic agent for breast cancer.

Introduction

The p90-kDa ribosomal S6 kinase (RSK) family is an important downstream effector of mitogen-activated protein kinase (MAPK). MAPK is known to be important in proliferation and oncogenesis.[1,2] However, it has not been possible to distinguish the function of RSK in these processes from those of MAPK itself and of the many other downstream MAPK effectors because until recently there have been no RSK-specific inhibitors.[3] We previously found that an extract from *Forsteronia refracta*, a member of the Apocynaceae (dogbane) family found in the South American rainforest, was able to specifically inhibit RSK catalytic activity.[3] Fractionation of the extract led to the isolation of an active component kaempferol 3-*O*-(3", 4"-di-*O*-acetyl-α-L-rhamnopyranoside), also referred to as SL0101 (Fig. 1).[3] SL0101 is competitive with respect to ATP with a dissociation constant, K_i, of 1 μM. This compound is an effective and extremely specific RSK inhibitor in intact cells. SL0101 inhibits proliferation of the human breast cancer cell line, MCF-7, with an efficacy paralleling its ability to inhibit RSK in intact cells. Significantly, SL0101 does not prevent the growth of the normal breast line, MCF-10A, even though it inhibits RSK activity in these cells. These results suggest that RSK may be an important novel drug target in some types of cancer and that SL0101 may be a useful chemotherapeutic agent.

In intact cells the IC_{50} of SL0101 for inhibition of RSK activity and MCF-7 cell proliferation is ~ 50 μM. Thus the potency of SL0101 as a RSK inhibitor in intact cells is 50-fold higher than the dissociation constant. Therefore, on the assumption that the potency of SL0101 in cells was limited by cellular uptake, we investigated the possibility of improving the potency of SL0101 by using a prodrug approach, which would not diminish the remarkable specificity of SL0101 for inhibiting RSK

catalytic activity. The total synthesis of the prodrug, kaempferol 3-*O*-(2",3","4"-tri-*O*-acetyl-α-L-rhamnopyranoside), referred to as 3Ac-SL0101, was performed. The synthesis of SL0101 or 3Ac-SL0101 has not previously been reported. We found that 3Ac-SL0101, like SL0101, is an effective and specific inhibitor of RSK activity in intact cells. 3Ac-SL0101 was ~2-fold more effective in inhibiting the growth of the MCF-7 line than SL0101. 3Ac-SL0101 also retained the remarkable ability to preferentially inhibit MCF-7 but not MCF-10A proliferation. Thus 3Ac-SL0101 is of interest for further characterization as a potential chemotherapeutic agent for breast cancer.

Results

To investigate the possibilities to improve the potency of SL0101 we characterized two compounds structurally related to SL0101 for their abilities to inhibit RSK activity. These compounds, kaempferol 3-*O*-(2", 4"-di-*O*-acetyl-α-L-rhamnopyranoside), 2",4" di-*O*-acetyl-SL0101, and kaempferol 3-*O*-(4"-mono-*O*-acetyl-α-L-rhamnopyranoside), 4" mono-*O*-acetyl-SL0101, differ from SL0101 in either the position or number of acetyl groups present on the rhamnose moiety (Fig. 1) and were obtained during the purification of SL0101 from *F. refracta*. The ability of the purified compounds to inhibit RSK activity was determined in an *in vitro* kinase assay using recombinant, constitutively active RSK2[3] (Fig. 2A). In this assay the IC_{50} values for SL0101 and 4" mono-*O*-acetyl-SL0101 are ~100 nM and ~200 nM, respectively, and for 2",4" di-*O*-acetyl-SL0101 the IC_{50} is ~ 500 nM. Thus all three related compounds are able to inhibit RSK catalytic activity *in vitro*. To determine whether the related compounds inhibit RSK activity in intact cells we examined their ability to inhibit the proliferation of MCF-7 cells. Previously we have shown that SL0101 inhibits MCF-7 proliferation by specifically inhibiting RSK activity.[3] SL0101 is able to inhibit MCF-7 proliferation with an EC_{50} of ~ 50 μM[3] and our current results are in agreement with those observations (Fig. 2B). SL0101 and 2",4"-di-*O*-acetyl-SL0101 at 50 μM were similarly effective at inhibiting MCF-7 growth. However, 4" mono-*O*-acetyl-SL0101 did not inhibit MCF-7 proliferation at 50 μM. These data show that the position of the acetyl groups is not particularly important in determining the *in vitro* affinity for RSK. However, a minimum of two acetyl groups appears to be required for inhibition of RSK activity in intact cells. It is likely that the acetyl groups are essential to allow effective uptake of the inhibitor into the cell.

Based on our results we reasoned that kaempferol 3-*O*-(2", 3,"4"-tri-*O*-acetyl-α-L-rhamnopyranoside)(3Ac-SL0101), would be a more potent inhibitor in cell-based assays due to greater hydrophobicity, with a calculated octanol-water partition coefficient, LogP, of 3.07 compared to 2.56 for SL0101. We further hypothesized that once inside the cell the acetyl groups on 3Ac-SL0101 may be hydrolyzed to produce di- and mono-acetylated kaempferol rhamnopyranosides, which are RSK-specific inhibitors. Thus, 3Ac-SL0101, like SL0101, should demonstrate the remarkable specificity for inhibition of RSK activity in an intact cell.

The synthetic strategy for the synthesis of 3Ac-SL0101 can be divided into three steps: synthesis of the kaempferol aglycone, choice of the protected rhamnose for the coupling, and coupling between the kaempferol aglycone and rhamnose moieties. The synthesis of 3Ac-SL0101 is depicted in Figure 3. The multi-step synthesis of 4',7-dibenzylkaempferol has been reported[4] as well as the selective protection of related flavones using the method of Jurd.[5] This method involves the peracetylation of the flavone, followed by selective benzylation of the 4' and 7 positions and hydrolysis of the 3 and 5-acetate groups. However, when applied to kaempferol this approach resulted in a mixture of 4',7-dibenzylkaempferol and a monobenzyl kaempferol derivative. As an alternative the direct benzylation of kaempferol was investigated using 2 equivalents of benzyl bromide and potassium carbonate in acetone at reflux. Under these conditions a readily separable mixture of **2** (31%) and **2a** (39%) was formed. The structure of **2** was confirmed by comparison with a sample made by one of the alternative routes and by NOE and COSY experiments. Moreover the undesired **2a** was readily hydrogenated to kaempferol **1** in 95% yield.

The glycosidation of 4',7-dibenzylkaempferol has been reported.[6-9] In addition glycosidation of related flavones with a variety of per-*O*-acetyl glycosyl bromides has been reported but the yield with the rhamnose derivative was significantly lower than with other examples.[10] Additionally, both anomeric rhannose derivatives can be produced; they are distinguishable by ^{1}H NMR.[3d] A wide range of conditions for the glycosidation was investigated but, at best, a 19% yield could be obtained. The product was characterized by ^{1}H NMR and shown to be solely the α-anomer. The deprotection of **3** proceeded smoothly to give 3Ac-SL0101 in 86% yield.

To determine whether 3Ac-SL0101 inhibits RSK in intact cells we examined the phosphorylation of elongation factor 2 (eEF2) in MCF-7 cells. eEF2 mediates the translocation step in mRNA translation. eEF2 activity is regulated by phosphorylation; the protein is inactivated by a highly specific kinase, EF2 kinase (EF2K). RSK phosphorylates and inactivates EF2K in response to mitogenic stimulation, which leads to a decrease in phosphorylation of eEF2.[11] Thus, under conditions such as serum deprivation, which leads to low RSK activity, eEF2 is phosphorylated by the active EF2K. However, stimulation of RSK activity by mitogens such as phorbol ester results in reduced phosphorylation of eEF2 due to inactivation of EF2K by RSK.

Therefore, the phosphorylation state of eEF2 during mitogenic stimulation is an indicator of RSK activity. Inhibiting RSK activity by inactivating upstream signaling events with U0126, a mitogen-activated protein kinase kinase (MEK) inhibitor, results in activation of EF2K and phosphorylation of eEF2 even in the presence of mitogenic stimuli.[11] It would be expected that treatment of cells with a RSK inhibitor would also result in phosphorylation of eEF2 even in the presence of mitogenic stimuli.

As seen in lanes 1 and 2 of Figure 4, phorbol dibutyrate (PDB) treatment of MCF-7 cells inactivated EF2K as determined by the reduced levels of phosphorylated eEF2. The levels of total eEF2 were not altered by PDB treatment. However, pre-incubation of cells with 50 μM 3Ac-SL0101 or 100 μM SL0101 eliminated PDB-induced eEF2K inactivation and the levels of phosphorylated eEF2 remained elevated. MCF-7 cells secrete paracrine factors that activate MAPK. U0126 treatment of serum-deprived cells demonstrates the level of eEF2 phosphorylation under conditions of basal MAPK activity (lane 5). We have previously demonstrated that SL0101 does not affect the activation of MAPK, as detected by the anti-active MAPK antibody. Here we show that 3Ac-SL0101 does not alter PDB-stimulated MAPK activation (Fig. 4). Therefore, 3Ac-SL0101, like SL0101, is a membrane-permeable RSK inhibitor active in intact cells and does not inhibit upstream kinases necessary for PDB-stimulated MAPK activation, namely MEK, Raf and protein kinase C (PKC).

To demonstrate that 3Ac-SL0101 functions as a RSK-specific inhibitor in intact cells we compared the phosphorylation patterns from MCF-7 cells pre-incubated with either 3Ac-SL0101 or SL0101 prior to stimulation with PDB. The lysates were immunoblotted with multiple phospho-specific antibodies (Fig. 5). We have demonstrated that SL0101 does not alter the phosphorylation patterns detected by these antibodies whereas changes are readily detected in cells treated with U0126 as well as protein kinase A (PKA) or PKC inhibitors.[3] The phosphorylation patterns from PDB-treated cells pre-incubated with vehicle or 3Ac-SL0101 were identical (Fig. 5). Thus, 3Ac-SL0101, like SL0101, does not inhibit the phosphorylation of substrates associated with kinase activity of PKA, PKC, or Akt. These data indicate that 3Ac-SL0101 demonstrates specificity for RSK in intact cells relative to these other AGC kinase family members.

To test our hypothesis that 3Ac-SL0101 would be a more potent inhibitor than SL0101 we determined the ability of 3Ac-SL0101 to inhibit the proliferation of MCF-7 cells (Fig. 6). 3Ac-SL0101 inhibited proliferation with an IC_{50} of 25 μM. This IC_{50} is ~ 2-fold lower than that for SL0101. 3Ac-SL0101 did not significantly inhibit the proliferation of the normal breast line MCF-10A at concentrations that effectively inhibited MCF-7 proliferation by > 80% (Fig. 6). Therefore, 3Ac-SL0101 demonstrated a modest improvement for inhibition of MCF-7 proliferation compared to SL0101 without altering the specificity for inhibition of RSK activity.

Discussion

In addition to inhibiting MCF-7 proliferation we have found that 3Ac-SL0101 specifically inhibits the growth of the prostate cancer cell lines, LNCaP and PC-3.[12] The molecular mechanism that results in RSK playing a dominant role in regulating proliferation in some cancer types has not yet been elucidated. It has been proposed that among the numerous events involved in tumorigenesis is an increased reliance on compromised signaling pathways as well as the dormancy of alternative signaling pathways.[13,14] Thus it appears that some cancers have become dependent on RSK activity, rendering the proliferation of these cells amenable to inhibition by a RSK-inhibitor such as 3Ac-SL0101. The growth of normal cells would presumably not be inhibited by 3Ac-SL0101 because intact signaling pathways provide numerous mechanisms for circumventing inhibition of a single signaling event. The synthesis of 3Ac-SL0101 will allow the evaluation of 3Ac-SL0101 as an agent for treating breast and prostate cancers

Materials and Methods

Kinase assays and MCF-7 cell culture were performed as previously described[3] with the exception that 0.05% Cremophor EL (Sigma) was used as vehicle in the proliferation assays. Cremophor increases the IC_{50} of the RSK inhibitors to a small degree but is necessary to maintain solubility of 2",3",4" Ac-SL0101 at high concentrations. Antibodies used on cell lysates included anti-pan-MAPK (610124) from BD Transduction Laboratories; anti-phospho-MAPK (#V8031) from Promega; anti-eEF2 (2332), anti-phospho-eEF2 (2331), anti-phospho-Akt Substrate (9611), anti-phospho-PKA Substrate (9621), and anti-phospho-PKC Substrate (2261) from Cell Signaling Technology.

Chemistry. Reagents and solvents were used as received from commercial suppliers. Thin layer chromatography (TLC) was performed using Analtech silica gel plates 60 F_{254} and visualized by UV light at 254 nm or Hanessian stain. ^{1}H NMR and ^{13}C NMR spectra were obtained on a Bruker Avance-300 spectrometer at 300 MHz and 75 MHz, respectively. Samples were dissolved in an appropriate deuterated solvent ($CDCl_3$ or DMSO-d_6). Proton and carbon chemical shifts are reported as parts per million (δ) relative to tetramethylsilane. Mass spectra were recorded on a Finnigan aQa Mass Spectrometer. Flash column chromatography was performed with flash-grade silica gel (EMD Chemicals, Inc., 40-63 μ). HPLC analyses were conducted using Agilent 1100 series (using the following conditions: Phenomenex Prodigy 5µ ODS (2) 150 x 4.6 mm column, 40% water containing 0.1% of TFA in acetonitrile, flow rate 1 mL/min, run time 30 min).

7,4'-Dibenzyloxy-3,5-dihydroxyflavone (2). A mixture of 1.0 g (3.49 mmol) of kaempferol, 2.41 g (17% mmol) of anhydrous K_2CO_3, and 1.19 g (6.99 mmol) of BnBr was heated at reflux in anhydrous acetone for 16 h. The resulting reaction mixture was cooled to room temperature and the volatile

components were removed under diminished pressure. The residue was dissolved in 250 mL of dichloromethane, washed successively with two 250-mL portions of 6 N HCl, 250 mL of water, and 100 mL of brine, then dried over Na_2SO_4 and concentrated under diminished pressure. Flash column chromatography of the residue using heptane and EtOAc as eluants (gradient elution: heptane _10% EtOAc in heptane) provided 7,4'-dibenzyloxy-3,5-dihydroxyflavone (**2**)[5] as a yellow solid: yield 460 mg (31%), and tri-*O*-benzylated product **2a**: yield 700 mg (39%); ^{1}H NMR (DMSO-d_6) δ 5.04 (s, 2H), 5.24 (s, 2H), 6.47 (d, 1H, *J* = 2.0 Hz), 6.83 (d, 1H, *J* = 2.0 Hz), 6.90 (apparent d, 2H, *J* = 8.9 Hz), 7.25-7.52 (m, 10H), 7.90 (apparent d, 2H, *J* = 8.9 Hz) and 10.26 (s, 1H); ^{13}C NMR (DMSO-d_6) δ 70.4, 73.8, 93.6, 98.8, 105.7, 115.8, 120.9, 128.2, 128.5, 128.6, 128.8, 128.9, 130.8, 136.5, 136.8, 136.9, 156.7, 157.1, 160.6, 161.4, 164.5 and 178.5; HPLC: t_R 24.38 min; mass spectrum, *m/z* 467.2 $[M + H]^+$, theoretical, *m/z* 467.1.

Tri-*O*-benzyl derivative **2a**: ^{1}H NMR ($CDCl_3$) δ 4.98 (s, 2H), 5.04 (s, 2H), 5.06 (s, 2H), 6.35 (d, 1H, *J* = 2.3 Hz), 6.40 (d, 1H, *J* = 2.3 Hz), 6.89-6.98 (apparent m), 7.12-7.41 (m, 15H), 7.84-7.93 (apparent m, 2H); mass spectrum, *m/z* 557.3 $[M + H]^+$, theoretical, *m/z* 557.2.

7,4'-Dibenzyloxy-3,5-dihydroxyflavone-3-*O*-(2",3",4"-tri-*O*-acetyl-α-L-rhamnopyranoside) (3). To a solution of 1.81 g (3.88 mmol) of 7,4'-di-*O*-benzyl-3,5-dihydroxyflavone in 30 mL of quinoline was added at 25 °C 3.88 g of anh. calcium sulfate, 0.89 g (3.22 mmol) of silver carbonate and, in two portions, 2.74 g (7.76 mmol) of 2,3,4-tri-O-acetyl-α-L-rhamnopyranosyl bromide.[15] The reaction mixture was stirred at room temperature for 16 h and diluted with 350 mL of dichloromethane. The solution was washed with two 250-mL portions of 6 N HCl, 250 mL of water, and 100 mL of brine, then dried over Na_2SO_4 and concentrated *in vacuo*. Unreacted starting material (1.6 g; 7,4'-

dibenzyloxy-3,5-dihydroxyflavone, **2**) was recovered by dissolving the crude product in 30 mL of dichloromethane followed by precipitation with 300 mL of heptane. After flash column chromatography of the mother liquors (gradient: toluene _ 5% ethanol in toluene), consumed 7,4'-dibenzyloxy-3,5-dihydroxyflavone-3-*O*-(2",3",4"-tri-*O*-acetyl-α-L-rhamnopyranoside) (**3**) was isolated as a colorless syrup: yield 65 mg (19% based on consumed starting material); ^{1}H NMR ($CDCl_3$) δ 1.45 (d, 3H, *J* = 6.2 Hz), 1.97 (s, 3H), 1.99 (s, 3H), 2.14 (s, 3H), 3.82-3.96 (m, 1H), 4.93-5.25 (m, 5H), 5.35-5.51 (m, 3H), 6.35 (d, 1H, *J* = 1.8 Hz), 6.42 (d, 1H, *J* = 1.8 Hz), 7.04 (d, 2H, *J* = 8.8 Hz), 7.13-7.38 (m, 10H) and 7.87 (d, 2H, *J* = 8.8 Hz); ^{13}C NMR ($CDCl_3$) δ 17.8, 21.0, 21.1, 21.2, 67.9, 69.2, 69.9, 70.9, 71.2, 74.8, 77.5, 93.5, 95.9, 99.1, 106.7, 116.4, 125.4, 127.8, 128.7, 129.1, 129.2, 130.9, 136.2, 136.7, 138.0, 165.6, 157.2, 157.9, 162.6, 164.9, 170.3, 170.4 and 179.3; *m/z* 739.2 $[M + H]^+$, theoretical, mass spectrum, *m/z* 739.2.

3,5,7,4'-Tetrahydroxyflavone-3-*O*-(2",3",4"-tri-*O*-acetyl-α-L-rhamnopyranoside) (4). To a solution of 325 mg (0.44 mmol) of 7,4'-dibenzyloxy-3,5-dihydroxyflavone-3-*O*-(2",3",4"-tri-*O*-acetyl-α-L-rhamnopyranoside) (**3**) in 20 mL of EtOAc was added 35 mg of 10% palladium on carbon at room temperature. The reaction mixture was stirred under a hydrogen atmosphere for 16 h. The reaction mixture was then filtered through a Celite pad and the pad was washed with 10 mL of EtOAc. Concentration of the combined filtrate under diminished pressure and purification of the residue by preparative TLC (5% ethanol in toluene) provided 3,5,7,4'-tetrahydroxyflavone-3-*O*-(2",3",4"-tri-*O*-acetyl-α-L-rhamnopyranoside) (**4**) as light yellow solid: yield 210 mg (86%); ^{1}H NMR ($CDCl_3$) δ 1.23 (d, 3H, *J* = 6.0 Hz), 2.09 (s, 3H), 2.10 (s, 3H), 2.25 (s, 3H), 3.92-4.07 (m, 1H), 5.21 (apparent t, 1H, *J* = 10.2 Hz), 5.48-5.63 (m, 3H), 6.10-6.89 (m, 3H), 7.15 (apparent s, 2H), 8.10 (apparent s, 2H) and 11.51-12.05 (m, 1H); ^{13}C NMR ($CDCl_3$) δ 17.8, 21.2, 21.3, 67.9, 69.4, 70.2, 71.3, 77.6, 94.6, 95.7,

99.2, 104.2, 116.6, 125.5, 129.7, 136.3, 145.3, 157.2, 157.4, 161.6, 162.9, 170.6, 170.8, 170.9 and 175.6; HPLC: t_R 4.35 min; mass spectrum, *m/z* 559.2 $[M + H]^+$; theoretical, *m/z* 559.1.

Acknowledgements

This work was by Department of Defense #DAMD17-03-1-0366 USAMRMC, by the Paul Mellon Prostate Cancer Institute and the Prostate Cancer Foundation (CaPCURE). The authors wish to thank the Patients and Friends of the Cancer Center and the University of Virginia Cancer Center for funding the development of the synthetic procedure.

References

(1) Roux, P. P.; Blenis, J. ERK and p38 MAPK-activated protein kinases: a family of protein kinases with diverse biological functions. *Microbiol Mol Biol Rev* **2004**, *68*, 320-344.

(2) Sebolt-Leopold, J. S. Development of anticancer drugs targeting the MAP kinase pathway. *Oncogene* **2000**, *19*, 6594-6595.

(3) Smith, J. A.; Poteet-Smith, C. E.; Xu, Y.; Errington, T. M.; Hecht, S. M. et al. Identification of the first inhibitor of p90 ribosomal S6 kinase (RSK) reveals an unexpected role for RSK in cancer cell proliferation. *Cancer Res.* **2005**, *65*, 1027-1034.

(4) Wagner, H.; Danninger, H.; Seligmann, O.; Nogradi, M.; Farkas, L. et al. [Synthesis of glucuronides in the flavonoid series. II. Isolation of kaempferol-3-beta-D-glucuronide from Euphorbia esula L]. *Chem Ber* **1970**, *103*, 3678-3683.

(5) Jurd, L. The selective alkylation of polyphenols. II. Methylation of 7'-,4'-, and 3'-hydroxyl groups in flavanol. *J. Org. Chem* **1962**, *27*, 1294-1297.

(6) Chari, V. M.; Wagner, H. Synthese von 3,4',5,7-tetrahydroxyflavon-3-*O*-(2-*O*-a-D-xylopyranosyl-b-D-glucopyranosid. *Chem. Ber.* **1976**, *109*, 426-432.

(7) Li, M.; Han, X.; Yu, B. Synthesis of quercitin 3-*O*-(2"-galloyl)-a-L-arabinopyranoside. *Tettrahedron Lett.* **2002**, *43*, 9467-9470.

(8) Farkas, L.; Vermes, B.; Mihaly, N.; Kalman, A. the synthesis of flavonol 3-O-b-gentriotriosides. *Phytochemistry* **1976**, *15*, 1184-1185.

(9) Vermes, B.; Farkas, L.; Nogradi, M.; Wagner, H.; Dirscherl, R. The synthesis of afzelin, paeonoside and kaempferol 3-*O*-b-rutinoside. *Phytochemistry* **1976**, *15*, 1320-1321.

(10) Demetzos, C.; Skaltsounis, A. L.; Tillequin, F.; Koch, M. Phase-transfer-catalyzed synthesis of flavonoid glycosides. *Carbohydr Res* **1990**, *207*, 131-137.

(11) Wang, X.; Li, W.; Williams, M.; Terada, N.; Alessi, D. R. et al. Regulation of elongation factor 2 kinase by p90(RSK1) and p70 S6 kinase. *Embo J* **2001**, *20*, 4370-4379.

(12) Clark, D. E.; Errington, T. M.; Smith, J. A.; Frierson, H. F., Jr.; Weber, M. J. et al. The serine/threonine protein kinase, p90 ribosomal S6 kinase, is an important regulator of prostate cancer cell proliferation. *Cancer Res* **2005**, *65*, 3108-3116.

(13) Mills, G. B.; Lu, Y.; Kohn, E. C. Linking molecular therapeutics to molecular diagnostics: Inhibition of the FRAP/RAFT/TOR component of the PI3K pathway preferentially blocks PTEN mutant cells in vitro and in vivo. *Proc. Natl. Acad. Sci. USA* **2001**, *98*, 10031-10033.

(14) Neshat, M. S.; Mellinghoff, I. K.; Tran, C.; Stiles, B.; Thomas, G. et al. Enhanced sensitivity of PTEN-deficient tumors to inhibition of FRAP/mTOR. *Proc. Natl. Acad. Sci. USA* **2001**, *98*, 10314-10319.

Figure Legends

Figure 1.

Structure of SL0101, 2",4" di-acetyl-SL0101 and 4" mono-acetyl-SL0101. These compounds differ in either the position or number of acetyl groups present on the rhamnose moiety. OH, hydroxyl; OAc, acetyl ester.

Figure 2.

Effect of SL0101, 2",4" di-acetyl-SL0101 and 4" mono-acetyl-SL0101 on RSK activity. ***A,*** The potency of purified compounds in inhibiting RSK catalytic activity was measured. Kinase assays were performed using immobilized substrate. The reactions were initiated by the addition of 10 μM ATP (final concentration). Reactions were terminated after 30 min. All assays measured the initial reaction velocity. The extent of phosphorylation was determined using phosphospecific antibodies in combination with HRP-conjugated secondary antibodies. HRP activity was measured as described in Materials and Methods. Maximum and minimum activity is the relative luminescence detected in the presence of vehicle and 200 mM EDTA, respectively. *Points*, mean (n = 2 in triplicate); *bars* = SD. ***B,*** The potency of purified compounds in inhibiting MCF-7 cell proliferation was determined. MCF-7 cells were treated with vehicle or 50 μM of SL0101, 2",4" di-acetyl-SL0101, or 4" mono-acetyl-SL0101 and cell viability was measured after 72 hr of treatment. Values given are the fold proliferation. *Points*, mean (n = 3 in quadruplicate); *bars* = SD.

Figure 3.

Synthesis of 3Ac-SL0101. Reagents and conditions: (a) K_2CO_3, BnBr, acetone, 57 C, 16 h; (b) 2,3,4-Tri-*O*-acetyl-α-L-rhamnopyranosyl bromide, Ag_2CO_3, $CaSO_4$, quinoline, 23 C, 16 h: (c) Pd/C, H_2, EtOAc, 23 C, 16h.

Figure 4.

3Ac-SL0101 is an effective RSK inhibitor in intact cells. Serum-deprived MCF-7 cells were pre-incubated with vehicle, 50 μM 3Ac-SL0101, 100 μM SL0101 or 25 μM U0126 for 3 hr. Cells were treated with 500 nM PDB or vehicle for 30 min prior to lysis. Protein concentration of lysates was measured and lysates were electrophoresed, transferred and immunoblotted. Equal loading of lysate is demonstrated by the anti-eEF2 and anti-pan-MAPK immunoblots.

Figure 5.

Comparison of the effect of 3Ac-SL0101 and SL0101 on phosphorylation patterns in intact cells. MCF-7 cell lysates previously normalized for protein concentration and equal loading as determined by eEF2 and anti-pan-MAPK immunoblotting (Fig 4) were electrophoresed, transferred and immunoblotted with anti-phospho-PKA substrate, anti-phospho PKC substrate or anti-phospho-Akt substrate.

Figure 6.

3Ac-SL0101 selectively inhibits MCF-7 cell proliferation. MCF-7 and MCF-10A cells were treated with vehicle or indicated concentration of 3Ac-SL0101 and cell viability was measured after 48 hr of

treatment. Values given are the fold proliferation as a percentage of that observed with vehicle-treated cells. *Points*, mean (n = 3 in quadruplicate); *bars* = SD.

Smith, *et al.*, Synthesis of 3AC-SL0101 FIGURE 1

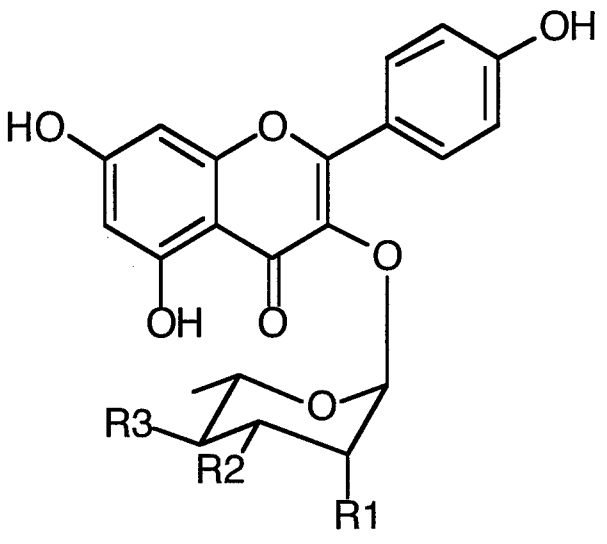

	R1	R2	R3
SL0101	OH	OAc	OAc
2",4" di-acetyl-SL0101	OAc	OH	OAc
4" mono-acetyl-SL0101	OH	OH	OAc

Smith, *et al.*, Synthesis of 3AC-SL0101

FIGURE 2

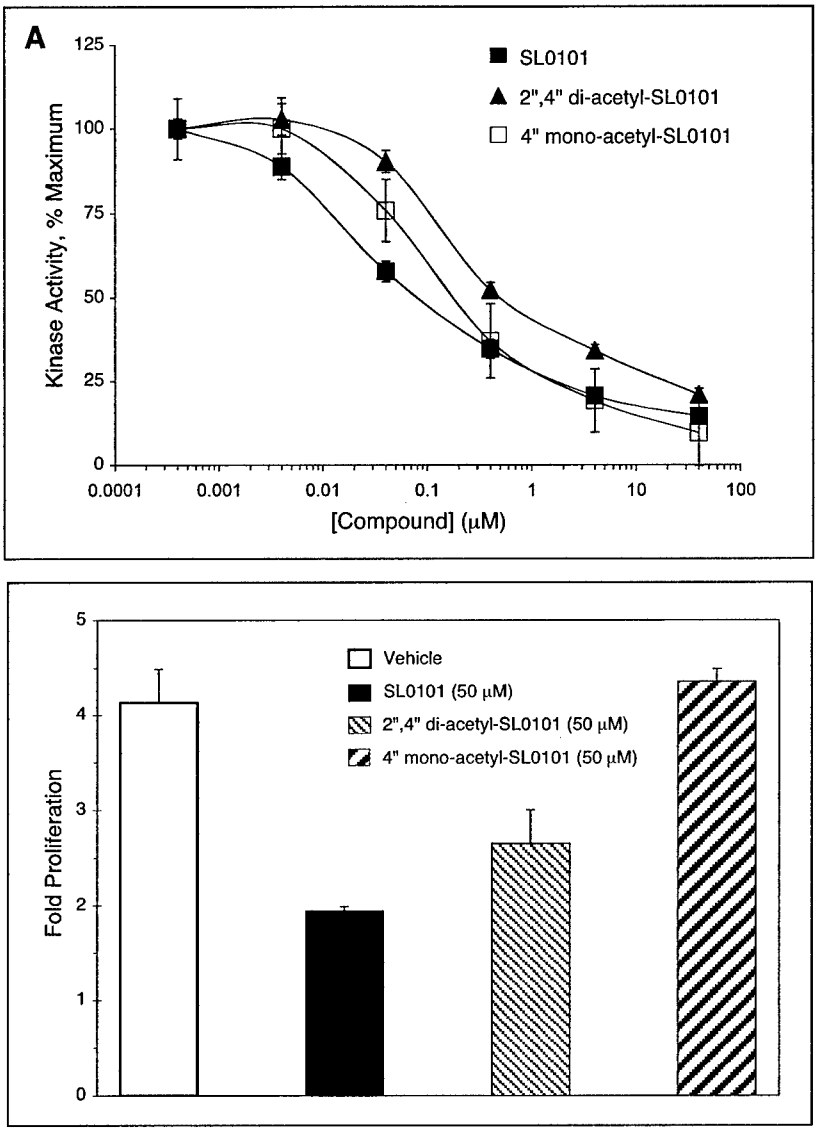

Smith, *et al.*, Synthesis of 3AC-SL0101

FIGURE 3

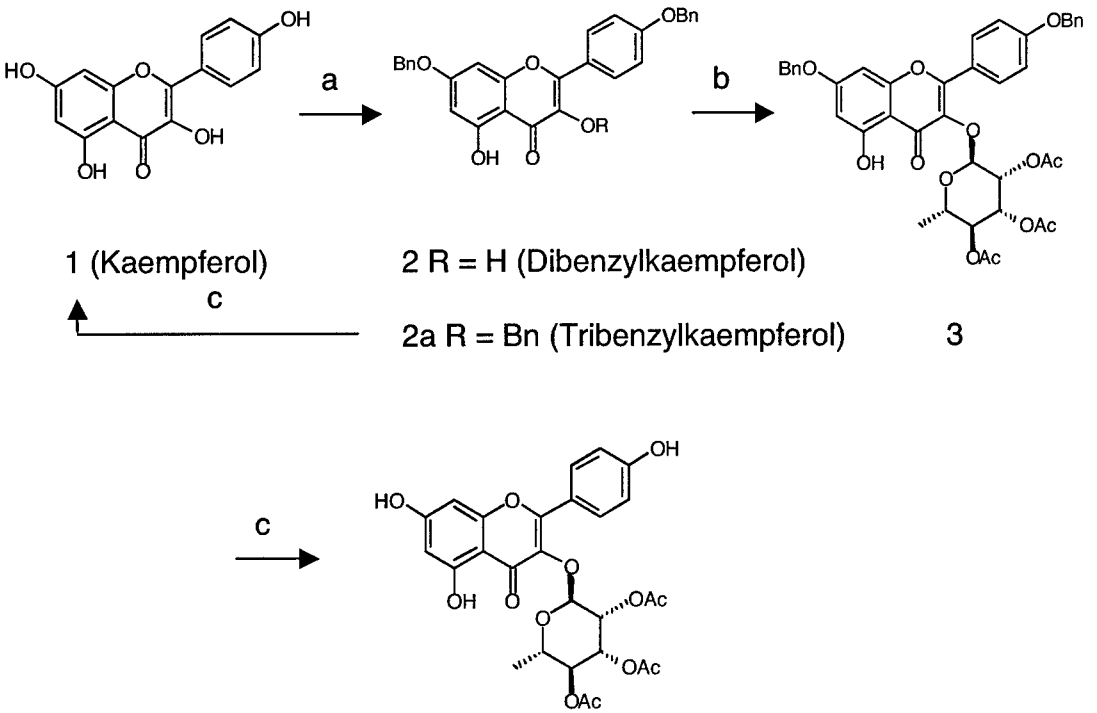

4

Smith, *et al.*, Synthesis of 3AC-SL0101 FIGURE 4

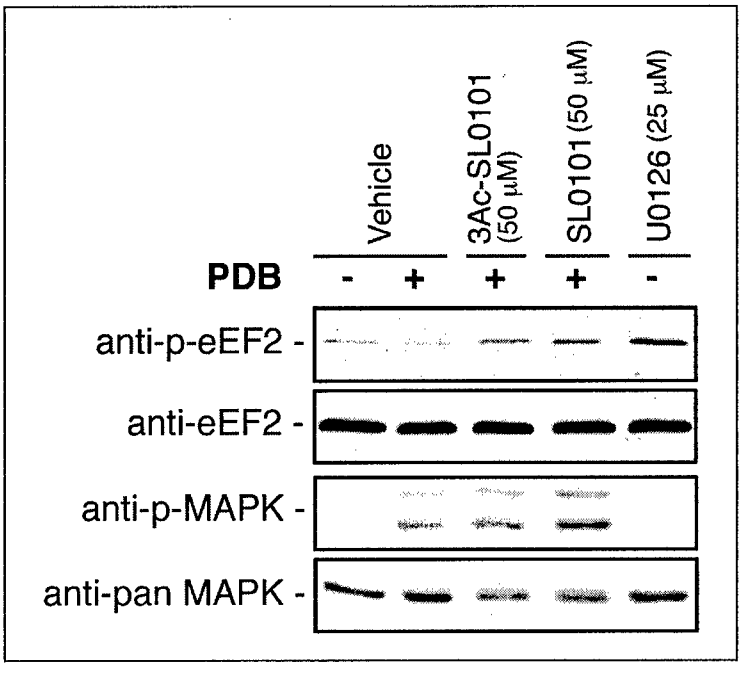

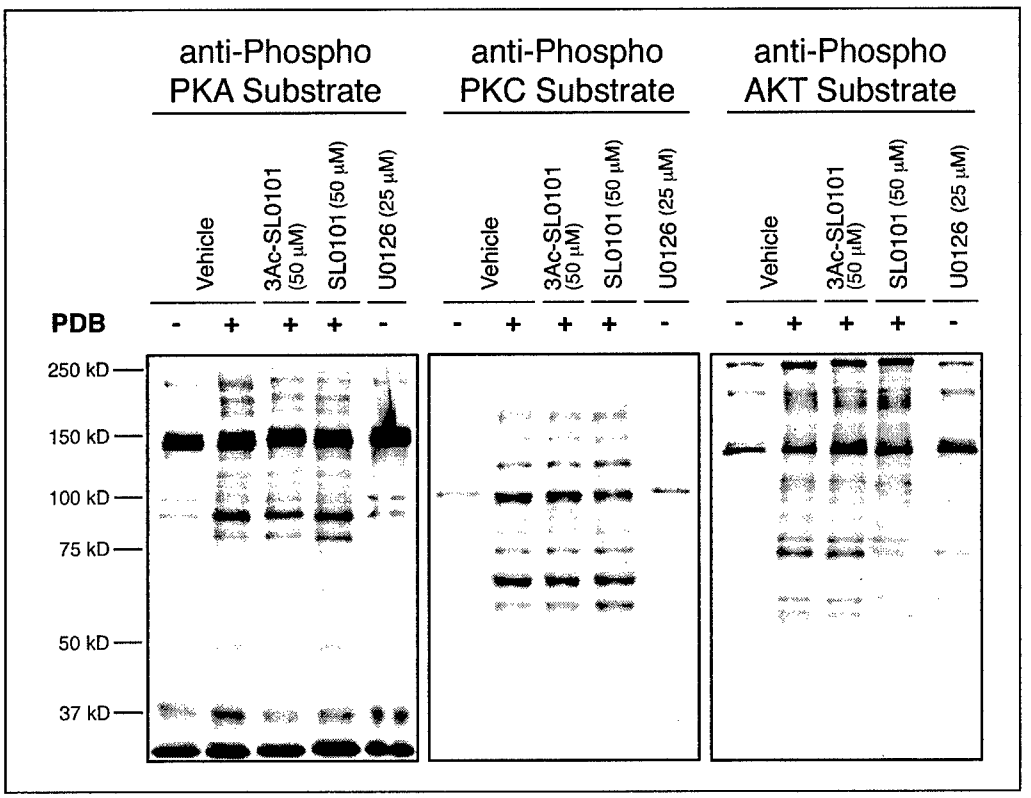
anti-Phospho PKA Substrate
anti-Phospho PKC Substrate
anti-Phospho AKT Substrate
Vehicle
3Ac-SL0101 (50 μM)
SL0101 (50 μM)
U0126 (25 μM)
PDB
- + + + -
250 kD
150 kD
100 kD
75 kD
50 kD
37 kD

Smith, *et al.*, Synthesis of 3AC-SL0101

FIGURE 6